

CONFIDENTIAL

RM A52L02



FEB 20 1953



# RESEARCH MEMORANDUM

LIFT, DRAG, AND PITCHING MOMENT OF LOW-ASPECT-RATIO WINGS  
AT SUBSONIC AND SUPERSONIC SPEEDS - COMPARISON OF THREE  
WINGS OF ASPECT RATIO 2 OF RECTANGULAR, SWEEPED-BACK,  
AND TRIANGULAR PLAN FORM, INCLUDING EFFECTS OF  
THICKNESS DISTRIBUTION

By Ronald C. Hightower

Ames Aeronautical Laboratory  
Moffett Field, Calif.

CLASSIFICATION CHANGED

UNCLASSIFIED

To \_\_\_\_\_

By authority of *NACA Re abs - Effective*  
*4 RN-114* Date *4-8-57*  
*NB 4-30-57*

CLASSIFIED DOCUMENT

This material contains information affecting the National Defense of the United States within the meaning of the espionage laws, Title 18, U.S.C., Secs. 793 and 794, the transmission or revelation of which in any manner to an unauthorized person is prohibited by law.

## NATIONAL ADVISORY COMMITTEE FOR AERONAUTICS

WASHINGTON

February 16, 1953

CONFIDENTIAL

NACA LIBRARY  
LANGLEY AERONAUTICAL LABORATORY  
Langley Field, Va.

NACA RM A52L02

~~CONFIDENTIAL~~

## NATIONAL ADVISORY COMMITTEE FOR AERONAUTICS

RESEARCH MEMORANDUM

LIFT, DRAG, AND PITCHING MOMENT OF LOW-ASPECT-RATIO WINGS  
AT SUBSONIC AND SUPERSONIC SPEEDS - COMPARISON OF THREE  
WINGS OF ASPECT RATIO 2 OF RECTANGULAR, SWEEPED-BACK,  
AND TRIANGULAR PLAN FORM, INCLUDING EFFECTS OF  
THICKNESS DISTRIBUTION

By Ronald C. Hightower

## SUMMARY

The aerodynamic characteristics of three wing-body combinations employing wings of aspect ratio 2, of rectangular, swept-back, and triangular plan form are compared at subsonic and supersonic speeds. All three wings had 3-percent-thick airfoil sections. The rectangular and swept-back wings were investigated with both biconvex and rounded-nose airfoil sections. The latter were obtained by replacing the portion of the biconvex sections forward of the midchord location with a semi-ellipse of minor axis equal to the airfoil maximum thickness. The triangular wing was composed of NACA 0003-63 airfoil sections.

The test Reynolds numbers were 1.8 million and 4.4 million for the rectangular wing, 1.9 million and 4.8 million for the swept-back wing, and 3.0 million and 7.5 million for the triangular wing. Most of the data were obtained in the range of Mach numbers from 0.61 to 0.93 and from 1.20 to 1.90. Data were not obtained for the complete Mach number range for the triangular wing and for the other wings at the higher Reynolds numbers.

The variation from rectangular to swept-back to triangular plan form influenced the aerodynamic characteristics in the following manner:

1. Reduced the lift-curve slope
2. Reduced the center-of-pressure travel with Mach number
3. Reduced the minimum drag coefficient at supersonic speeds
4. Increased the maximum lift-drag ratio at supersonic speeds

The airfoil-section thickness distribution had a significant effect on the drag characteristics of the rectangular and swept-back wings.

~~CONFIDENTIAL~~

The minimum drag coefficients of the wings with rounded-nose sections were lower than those of the wings with biconvex sections at all subsonic speeds and at supersonic speeds for which the Mach number is less than that for the attachment of the bow wave to the sharp leading edge of the biconvex section.

## INTRODUCTION

A research program is in progress at the Ames Aeronautical Laboratory to ascertain experimentally at subsonic and supersonic Mach numbers the aerodynamic characteristics of wings of interest in the design of high-speed airplanes. The effects of variations in plan form, twist, camber, and thickness are being investigated. The results of this program to date are presented in references 1 to 16. These results showed that plan form was one of the primary factors influencing the characteristics of wings in the high-subsonic and supersonic speed ranges. This report compares three wings of aspect ratio 2 of rectangular, swept-back, and triangular<sup>1</sup> plan form. The effects of modifying biconvex airfoil sections to rounded-nose airfoil sections on the characteristics of the rectangular and swept-back wings are also presented.

## NOTATION

b	wing span
$\bar{c}$	mean aerodynamic chord, $\frac{\int_0^{b/2} c^2 dy}{\int_0^{b/2} c dy}$
c	local wing chord
l	length of body including portion removed to accommodate sting
L/D	lift-drag ratio
$(L/D)_{\max}$	maximum lift-drag ratio
M	Mach number
q	free-stream dynamic pressure

---

<sup>1</sup>Data for the triangular wing were presented in reference 1.

---

R	Reynolds number based on the mean aerodynamic chord
r	radius of body
$r_0$	maximum body radius
S	total wing area, including area formed by extending leading and trailing edges to plane of symmetry
x	longitudinal distance from nose of body
y	spanwise distance from the vertical plane of symmetry
$\alpha$	angle of attack of body axis, deg
$C_D$	drag coefficient, drag/qS
$C_{D_{min}}$	minimum drag coefficient
$C_L$	lift coefficient, lift/qS
$C_m$	pitching-moment coefficient referred to quarter point of mean aerodynamic chord, pitching moment/qS $\bar{c}$
$\frac{dC_L}{d\alpha}$	slope of the lift curve measured in the range of lift coefficients from -0.1 to +0.1

#### APPARATUS

##### Wind Tunnel and Equipment

The experimental investigation was conducted in the Ames 6- by 6-foot supersonic wind tunnel. In this wind tunnel, the Mach number can be varied continuously and the stagnation pressure can be regulated to maintain a given test Reynolds number. The air is dried to prevent formation of condensation shocks. Further information on this wind tunnel is presented in reference 17.

The models were sting mounted in the tunnel, the diameter of the sting being about 93 percent of the diameter of the body base. The pitch plane of the model support was horizontal. The 4-inch-diameter, four-component, strain-gage balance, described in reference 18, was enclosed within the bodies of the models and was used to measure the aerodynamic forces and moments.

## Models

Plan and front views of the models and certain model dimensions are given in figure 1. (The dimensions of the triangular-wing model of ref. 1 are also given for convenience.) The biconvex profile and the rounded-nose modification of the rectangular and swept-back wings are illustrated in figure 2. The triangular wing was constructed of solid steel. The basic rectangular and swept-back wings with biconvex sections were also of steel, and were modified by adding bismuth-tin alloy forward of the midchord locations to obtain the rounded-nose sections. The profile of the rounded-nose section forward of the midchord location was elliptical; the tangent to the airfoil section at the midchord location was horizontal. The bodies used in the tests were constructed of steel and aluminum. The surfaces of the bodies and wings were polished smooth. Other geometric characteristics of the models are tabulated as follows:

Wings			
Wing plan form	Rectangular	Swept back	Triangular
Aspect ratio	2	2	2
Taper ratio	1	0.333	0
Sweepback of leading edge, deg	0	45	63.4
Total area, S, sq ft	2.425	2.425	4.014
Mean aerodynamic chord, $\bar{c}$ , ft	1.102	1.195	1.889
Dihedral, deg	0	0	0
Camber	None	None	None
Twist, deg	0	0	0
Incidence, deg	0	0	0
Distance, wing-chord plane to body axis, ft	0	0	0
Airfoil section (streamwise)	3% thick, biconvex	3% thick, biconvex	NACA 0003-63
	3% thick, rounded nose	3% thick, rounded nose	

Bodies			
Wing plan form	Rectangular	Swept back	Triangular
Fineness ratio (based upon length $l$ , fig. 1)	12.5	12.5	12.5
Cross-section shape	Circular	Circular	Circular
Maximum cross-sectional area, sq ft	0.123	0.123	0.204
Ratio of maximum cross-sectional area to wing area	0.0509	0.0509	0.0509

### TESTS AND PROCEDURE

#### Range of Test Variables

The lift, drag, and pitching moment of the models were measured at angles of attack from approximately  $-4^{\circ}$  to  $+17^{\circ}$ . The results were obtained at Reynolds numbers of 1.8 million and 4.4 million for the rectangular wing, 1.9 million and 4.8 million for the swept-back wing, and 3.0 million and 7.5 million for the triangular wing. Data for the rectangular and swept-back wings at the lower Reynolds numbers were obtained at Mach numbers from 0.61 to 0.93 and from 1.20 to 1.90. The rest of the data did not cover the complete Mach number range because of either electrical power limitations of the wind tunnel or choking effects of the model on the air stream in the test section.

#### Reduction of Data

The test data have been reduced to standard NACA coefficient form. Factors which could affect the accuracy of these results, together with the corrections applied, are discussed in the following paragraphs.

Tunnel-wall interference.— Corrections to the subsonic results for the induced effects of the tunnel walls resulting from lift on the models were made according to the methods of reference 19. The numerical values of these corrections (which were added to the uncorrected data) were:

Wing plan form	Rectangular	Swept back	Triangular
$\Delta\alpha$	$0.55 C_L$	$0.55 C_L$	$0.93 C_L$
$\Delta C_D$	$.0095 C_L^2$	$.0095 C_L^2$	$.016 C_L^2$

No corrections were made to the pitching-moment coefficients.

The effects of constriction of the flow at subsonic speeds by the tunnel walls were taken into account by the method of reference 20. This correction was calculated for conditions at zero angle of attack and was applied throughout the angle-of-attack range. At a Mach number of 0.91, the increase in the Mach number over that determined from a calibration of the wind tunnel without a model in place was 4 percent for the triangular wing model and 2 percent for the rectangular and swept-back-wing models.

For the tests at supersonic speeds, the reflection from the tunnel walls of the Mach wave originating at the nose of the body did not cross the model. No corrections were required, therefore, for tunnel-wall effects.

Stream variations.- Tests of the triangular wing of reference 1 in both the normal and inverted positions showed no stream curvature or inclination. Tests of the rectangular and swept-back wings in both the normal and inverted positions have indicated a maximum apparent stream inclination of approximately  $-0.1^\circ$ . The measured values of the apparent stream inclination were not consistent and, since unknown factors contributed to this effect, no corrections were made to the data of this report. The effects of stream curvature and stream inclination in the yaw plane of the models are not known, but are judged to be small according to the results of reference 21.

A survey of the air stream at subsonic and supersonic speeds has shown that there is a static-pressure variation in the test section of sufficient magnitude to affect the drag results. Corrections were added to the measured drag coefficients, therefore, to account for the longitudinal buoyancy caused by this static-pressure variation. These corrections varied from  $-0.0008$  to  $+0.0009$ .

Support interference.- At subsonic speeds, the effects of support interference on the aerodynamic characteristics of the models are not known. For the present tailless models, it is believed that such effects consisted primarily of a change in the pressure at the base of the model fuselage. In an effort to correct at least partially for this support interference, the base pressure of the model fuselage was measured and

the drag data were adjusted to correspond to a base pressure equal to the static pressure of the free stream.

At supersonic speeds, the effects of support interference of a body-sting configuration similar to that of the present models are shown by reference 22 to be confined to a change in base pressure. The previously mentioned adjustment of the drag for base pressure, therefore, was applied at supersonic speeds.

## RESULTS AND DISCUSSION

The lift, drag, and pitching-moment coefficients (for various angles of attack) for the rectangular and swept-back wing models, as well as for the triangular wing model<sup>2</sup> of reference 1, are presented in tables I to V. A summary of the aerodynamic characteristics of the models at the higher Reynolds numbers is presented in figure 3. The effects of Reynolds number are shown in figures 4, 5, 6, and 7. Pitching-moment curves for some subsonic Mach numbers at the lower Reynolds numbers were irregular through zero lift and the center-of-pressure locations for these Mach numbers are not presented.

### Effects of Wing Plan Form

In the following discussion of the effects of wing plan form on various aerodynamic parameters, wings with similar thickness distributions are compared. The triangular wing having an NACA 0003-63 section is compared with the rectangular and swept-back wings having rounded-nose sections.

Variations in plan form affected the lift-curve slopes at supersonic speeds more than at subsonic speeds (fig. 3(a)). As the Mach number increased in the supersonic speed range, the lift-curve slopes approached a constant value. For these three wings of the same aspect ratio, the lift-curve slope decreased as the leading-edge sweepback increased. At subsonic speeds, the lift curves for the rectangular and swept-back wings were nonlinear for lift coefficients greater than 0.1. The lift-curve slopes for these wings increased until a lift coefficient of approximately

---

<sup>2</sup>The subsonic results of reference 1 have been corrected for Mach number, dynamic pressure, and base drag according to the results of a survey of the air stream in the Ames 6- by 6-foot supersonic wind tunnel performed after the publication of reference 1. A buoyancy correction was also computed and added to the subsonic results.

---

0.7 was reached, then decreased at higher lift coefficients. The lift curves for the triangular wing were linear at all Mach numbers.

The variation from rectangular to swept-back to triangular plan form reduced the variation of the center-of-pressure location (in percent of mean aerodynamic chord) with Mach number (fig. 3(b)). For these three wings, even though the length of the mean aerodynamic chord increased as the sweepback increased, the travel of the center of pressure in actual dimension was least for the wing of greatest sweepback. At subsonic speeds, the pitching-moment curves for the rectangular and swept-back wings were nonlinear for lift coefficients greater than 0.1. The center-of-pressure location for these wings moved rearward as the lift coefficient increased. The pitching-moment curves for the triangular wing were linear for all Mach numbers.

The minimum drag coefficient at supersonic speeds (fig. 3(c)) was reduced by increasing the leading-edge sweepback. No general trends were concluded at subsonic speeds since any variations with changes in plan form were probably less than those caused by differences between the thickness distributions of the NACA 0003-63 section and the rounded-nose section and by differences in the amount of wing area enclosed within the fuselage.

The decrease of minimum drag at supersonic speeds with increasing sweepback angle was reflected in higher maximum lift-drag ratios (fig. 3(d)). The decrease of minimum drag more than offset the effect of the small decrease in lift-curve slope with increasing sweepback angle. At subsonic speeds, the effect of plan form on the maximum lift-drag ratio was opposite to that at supersonic speeds. The decrease of lift which resulted from an increase in the sweepback angle contributed the major effect and caused a decrease in the maximum lift-drag ratio.

#### Effects of Airfoil-Section Thickness Distribution

Replacing the biconvex sections of the rectangular and swept-back wings with rounded-nose sections caused only slight differences in the lift-curve slopes and center-of-pressure locations (figs. 3(a) and 3(b)).

The minimum drag at subsonic speeds of both the rectangular and swept-back wings was lower with the rounded-nose sections than with the biconvex sections (fig. 3(c)). The lower drag of the rounded-nose section resulted in higher maximum lift-drag ratios (fig. 3(d)). At supersonic speeds, the drag of the wings with rounded leading edges became higher at a Mach number of about 1.2 on the rectangular wing and (using lower Reynolds number data of figs. 6(a) and (b)) at a Mach number of 1.7 on the swept-back wing. It is estimated that these Mach numbers correspond

very nearly to the Mach numbers required for attachment of the bow shock wave on the sharp leading edges. In general, at supersonic speeds, the drag of sharp-leading-edge wings with detached bow waves might be expected to be greater than that of rounded-leading-edge wings.

### Effects of Reynolds Number

Small increases in the lift-curve slopes of both the rectangular and swept-back wings were obtained in the subsonic speed range by increasing the Reynolds number (fig. 4). No consistent viscous effects on lift-curve slope were evident at supersonic speeds.

The effect of Reynolds number on the center-of-pressure locations of the models was greater at subsonic speeds than at supersonic speeds (fig. 5). The effects were slight, however, and no consistent variations with Mach number were evident.

The minimum drag coefficients of the models varied consistently with Reynolds number (fig. 6). For all models, an increase in Reynolds number caused an increase in drag. This was attributed to the larger areas of turbulent boundary layer at the higher Reynolds numbers and the accompanying increased skin-friction drag of the turbulent boundary layer.

The lower minimum drag of the wings with sharp leading edges at the lower Reynolds numbers shown in figure 6(a) was reflected in the higher maximum lift-drag ratios shown in figure 7(a). The wings with rounded leading edges also showed lower minimum drag at the lower Reynolds numbers (fig. 6(b)), but an examination of the data showed a higher drag due to lift at the lower Reynolds numbers. This resulted in a slightly lower maximum lift-drag ratio at subsonic speeds for both wings with rounded leading edges at the lower Reynolds numbers (fig. 7(b)). For these wings, the effects at supersonic speeds were slight, and not as consistent as those at subsonic speeds.

### CONCLUSIONS

From the preceding discussion of the effects of plan form on the aerodynamic characteristics of three wings of aspect ratio 2 at subsonic and supersonic speeds, it is shown that variation in plan form from rectangular to swept back to triangular produces the following effects:

1. Reduces the lift-curve slope
2. Reduces the center-of-pressure travel with Mach number

3. Reduces the minimum drag coefficient at supersonic speeds
4. Increases the maximum lift-drag ratio at supersonic speeds

The minimum drag coefficients of wings at subsonic and supersonic speeds were found to be significantly affected by airfoil-section thickness distribution. The rounded-nose airfoil sections had less drag than biconvex airfoil sections at all subsonic speeds and at supersonic speeds for which the Mach number was less than that for the attachment of the bow wave to the sharp leading edge of the biconvex section.

Ames Aeronautical Laboratory  
National Advisory Committee for Aeronautics  
Moffett Field, California

#### REFERENCES

1. Heitmeyer, John C., and Smith, Willard G.: Lift, Drag, and Pitching Moment of Low-Aspect-Ratio Wings at Subsonic and Supersonic Speeds - Plane Triangular Wing of Aspect Ratio 2 With NACA 0003-63 Section. NACA RM A50K24a, 1951.
2. Smith, Donald W., and Heitmeyer, John C.: Lift, Drag, and Pitching Moment of Low-Aspect-Ratio Wings at Subsonic and Supersonic Speeds - Plane Triangular Wing of Aspect Ratio 2 With NACA 0008-63 Section. NACA RM A50K20, 1951.
3. Smith, Donald W., and Heitmeyer, John C.: Lift, Drag, and Pitching Moment of Low-Aspect-Ratio Wings at Subsonic and Supersonic Speeds - Plane Triangular Wing of Aspect Ratio 2 With NACA 0005-63 Section. NACA RM A50K21, 1951.
4. Heitmeyer, John C., and Stephenson, Jack D.: Lift, Drag, and Pitching Moment of Low-Aspect-Ratio Wings at Subsonic and Supersonic Speeds - Plane Triangular Wing of Aspect Ratio 4 With NACA 0005-63 Section. NACA RM A50K24, 1951.
5. Phelps, E. Ray, and Smith, Willard G.: Lift, Drag, and Pitching Moment of Low-Aspect-Ratio Wings at Subsonic and Supersonic Speeds - Triangular Wing of Aspect Ratio 4 With NACA 0005-63 Thickness Distribution, Cambered and Twisted for Trapezoidal Span Load Distribution. NACA RM A50K24b, 1951.

6. Smith, Willard G., and Phelps, E. Ray: Lift, Drag, and Pitching Moment of Low-Aspect-Ratio Wings at Subsonic and Supersonic Speeds - Triangular Wing of Aspect Ratio 2 With NACA 0005-63 Thickness Distribution, Cambered and Twisted for A Trapezoidal Span Load Distribution. NACA RM A50K27a, 1951.
7. Reese, David E., and Phelps, E. Ray: Lift, Drag, and Pitching Moment of Low-Aspect-Ratio Wings at Subsonic and Supersonic Speeds - Plane Tapered Wing of Aspect Ratio 3.1 With 3-Percent-Thick, Biconvex Section. NACA RM A50K28, 1951.
8. Hall, Charles F., and Heitmeyer, John C.: Lift, Drag, and Pitching Moment of Low-Aspect-Ratio Wings at Subsonic and Supersonic Speeds - Twisted and Cambered Triangular Wing of Aspect Ratio 2 With NACA 0003-63 Thickness Distribution. NACA RM A51E01, 1951.
9. Heitmeyer, John C.: Lift, Drag, and Pitching Moment of Low-Aspect-Ratio Wings at Subsonic and Supersonic Speeds - Plane Triangular Wing of Aspect Ratio 4 With 3-Percent-Thick, Biconvex Section. NACA RM A51D30, 1951.
10. Heitmeyer, John C., and Hightower, Ronald C.: Lift, Drag, and Pitching Moment of Low-Aspect-Ratio Wings at Subsonic and Supersonic Speeds - Plane Triangular Wing of Aspect Ratio 4 With 3-Percent-Thick Rounded-Nose Section. NACA RM A51F21, 1951.
11. Heitmeyer, John C.: Lift, Drag, and Pitching Moment of Low-Aspect-Ratio Wings at Subsonic and Supersonic Speeds - Plane Triangular Wing of Aspect Ratio 3 With NACA 0003-63 Section. NACA RM A51H02, 1951.
12. Heitmeyer, John C.: Lift, Drag, and Pitching Moment of Low-Aspect-Ratio Wings at Subsonic and Supersonic Speeds - Plane  $45^\circ$  Swept-Back Wing of Aspect Ratio 3, Taper Ratio 0.4 With 3-Percent-Thick, Biconvex Section. NACA RM A51H10, 1951.
13. Heitmeyer, John C.: Lift, Drag, and Pitching Moment of Low-Aspect-Ratio Wing at Subsonic and Supersonic Speeds - Body of Revolution. NACA RM A51H22, 1951.
14. Heitmeyer, John C., and Petersen, Robert B.: Lift, Drag, and Pitching Moment of Low-Aspect-Ratio Wings at Subsonic and Supersonic Speeds - Twisted and Cambered Triangular Wing of Aspect Ratio 2 With NACA 0005-63 Thickness Distribution. NACA RM A52B08, 1952.

15. Conrard, Donald: Lift, Drag, and Pitching Moment of Low-Aspect-Ratio Wings at Subsonic and Supersonic Speeds - Plane Triangular Wing of Aspect Ratio 3 With Air-to-Air Missile Models Mounted Externally. NACA RM A52C10a, 1952.
16. Heitmeyer, John C.: Lift, Drag, and Pitching Moment of Low-Aspect-Ratio Wings at Subsonic and Supersonic Speeds - Plane Tapered Wing of Aspect Ratio 3.1 With 3-Percent-Thick Rounded-Nose Section. NACA RM A52D23, 1952.
17. Frick, Charles W., and Olson, Robert N.: Flow Studies in the Asymmetric Adjustable Nozzle of the Ames 6- by 6-Foot Supersonic Wind Tunnel. NACA RM A9E24, 1949.
18. Olson, Robert N., and Mead, Merrill H.: Aerodynamic Study of a Wing-Fuselage Combination Employing a Wing Swept Back  $63^{\circ}$  - Effectiveness of an Elevon as a Longitudinal Control and the Effects of Camber and Twist on the Maximum Lift-Drag Ratio at Supersonic Speeds. NACA RM A50A31a, 1950.
19. Silverstein, Abe, and White, James A.: Wind-Tunnel Interference With Particular Reference to Off-Center Positions of the Wing and to the Downwash at the Tail. NACA Rep. 547, 1935.
20. Herriot, John G.: Blockage Corrections for Three-Dimensional-Flow Closed-Throat Wind Tunnels, With Consideration of the Effect of Compressibility. NACA Rep. 995, 1950. (Supercedes NACA RM A7B28).
21. Lessing, Henry C.: Aerodynamic Study of a Wing-Fuselage Combination Employing a Wing Swept Back  $63^{\circ}$  - Effect of Sideslip on Aerodynamic Characteristics at a Mach Number of 1.4 With the Wing Twisted and Cambered. NACA RM A50F09, 1950.
22. Perkins, Edward W.: Experimental Investigation of the Effects of Support Interference on the Drag of Bodies of Revolution at a Mach Number of 1.5. NACA TN 2292, 1951.

TABLE I.- AERODYNAMIC CHARACTERISTICS OF THE RECTANGULAR WING WITH 3-PERCENT-THICK BICONVEX SECTION

$\alpha$	$C_L$	$C_D$	$C_m$	$\alpha$	$C_L$	$C_D$	$C_m$	$\alpha$	$C_L$	$C_D$	$C_m$	$\alpha$	$C_L$	$C_D$	$C_m$	$\alpha$	$C_L$	$C_D$	$C_m$
M=0.61 R=1.8x10 <sup>6</sup>				M=0.71 R=1.8x10 <sup>6</sup>				M=0.81 R=1.8x10 <sup>6</sup>				M=0.91 R=1.8x10 <sup>6</sup>				M=1.00 R=1.8x10 <sup>6</sup>			
-0.27	-0.024	0.0099	0	-0.28	-0.022	0.0107	-0.001	-0.28	-0.020	0.0105	-0.003	-0.28	-0.018	0.0100	-0.006	-0.28	-0.016	0.0099	-0.008
-0.30	-0.034	0.0096	-0.002	-0.30	-0.033	0.0100	-0.003	-0.30	-0.031	0.0100	-0.006	-0.30	-0.029	0.0100	-0.010	-0.30	-0.028	0.0102	-0.011
-0.32	-0.044	0.0096	-0.004	-0.32	-0.046	0.0097	-0.005	-0.32	-0.046	0.0095	-0.008	-0.32	-0.046	0.0100	-0.012	-0.32	-0.046	0.0106	-0.013
-1.07	-0.62	0.100	-0.005	-1.08	-0.61	0.0996	-0.007	-1.08	-0.61	0.0992	-0.009	-1.08	-0.61	0.0986	-0.011	-1.08	-0.61	0.0980	-0.013
-2.15	-1.17	0.123	-0.009	-2.17	-1.16	0.126	-0.012	-2.19	-1.20	0.128	-0.016	-2.19	-1.23	0.128	-0.020	-2.20	-1.28	0.128	-0.026
-3.63	-1.74	0.157	-0.013	-3.65	-1.81	0.172	-0.016	-3.65	-1.87	0.182	-0.021	-3.61	-1.97	0.176	-0.031	-3.61	-1.99	0.179	-0.033
-4.30	-2.06	0.200	-0.016	-4.33	-2.06	0.203	-0.020	-4.30	-2.07	0.205	-0.026	-4.30	-2.08	0.204	-0.034	-4.32	-2.07	0.202	-0.031
-5.00	-2.25	0.246	-0.021	-5.00	-2.25	0.246	-0.021	-5.00	-2.25	0.246	-0.021	-5.00	-2.25	0.246	-0.021	-5.00	-2.25	0.246	-0.021
-5.80	-2.41	0.290	-0.025	-5.80	-2.41	0.290	-0.025	-5.80	-2.41	0.290	-0.025	-5.80	-2.41	0.290	-0.025	-5.80	-2.41	0.290	-0.025
-6.60	-2.56	0.334	-0.029	-6.60	-2.56	0.334	-0.029	-6.60	-2.56	0.334	-0.029	-6.60	-2.56	0.334	-0.029	-6.60	-2.56	0.334	-0.029
-7.40	-2.71	0.378	-0.033	-7.40	-2.71	0.378	-0.033	-7.40	-2.71	0.378	-0.033	-7.40	-2.71	0.378	-0.033	-7.40	-2.71	0.378	-0.033
-8.20	-2.86	0.422	-0.037	-8.20	-2.86	0.422	-0.037	-8.20	-2.86	0.422	-0.037	-8.20	-2.86	0.422	-0.037	-8.20	-2.86	0.422	-0.037
-9.00	-3.01	0.466	-0.041	-9.00	-3.01	0.466	-0.041	-9.00	-3.01	0.466	-0.041	-9.00	-3.01	0.466	-0.041	-9.00	-3.01	0.466	-0.041
-9.80	-3.16	0.510	-0.045	-9.80	-3.16	0.510	-0.045	-9.80	-3.16	0.510	-0.045	-9.80	-3.16	0.510	-0.045	-9.80	-3.16	0.510	-0.045
-10.60	-3.31	0.554	-0.049	-10.60	-3.31	0.554	-0.049	-10.60	-3.31	0.554	-0.049	-10.60	-3.31	0.554	-0.049	-10.60	-3.31	0.554	-0.049
-11.40	-3.46	0.598	-0.053	-11.40	-3.46	0.598	-0.053	-11.40	-3.46	0.598	-0.053	-11.40	-3.46	0.598	-0.053	-11.40	-3.46	0.598	-0.053
-12.20	-3.61	0.642	-0.057	-12.20	-3.61	0.642	-0.057	-12.20	-3.61	0.642	-0.057	-12.20	-3.61	0.642	-0.057	-12.20	-3.61	0.642	-0.057
-13.00	-3.76	0.686	-0.061	-13.00	-3.76	0.686	-0.061	-13.00	-3.76	0.686	-0.061	-13.00	-3.76	0.686	-0.061	-13.00	-3.76	0.686	-0.061
-13.80	-3.91	0.730	-0.065	-13.80	-3.91	0.730	-0.065	-13.80	-3.91	0.730	-0.065	-13.80	-3.91	0.730	-0.065	-13.80	-3.91	0.730	-0.065
-14.60	-4.06	0.774	-0.069	-14.60	-4.06	0.774	-0.069	-14.60	-4.06	0.774	-0.069	-14.60	-4.06	0.774	-0.069	-14.60	-4.06	0.774	-0.069
-15.40	-4.21	0.818	-0.073	-15.40	-4.21	0.818	-0.073	-15.40	-4.21	0.818	-0.073	-15.40	-4.21	0.818	-0.073	-15.40	-4.21	0.818	-0.073
-16.20	-4.36	0.862	-0.077	-16.20	-4.36	0.862	-0.077	-16.20	-4.36	0.862	-0.077	-16.20	-4.36	0.862	-0.077	-16.20	-4.36	0.862	-0.077
-17.00	-4.51	0.906	-0.081	-17.00	-4.51	0.906	-0.081	-17.00	-4.51	0.906	-0.081	-17.00	-4.51	0.906	-0.081	-17.00	-4.51	0.906	-0.081
-17.80	-4.66	0.950	-0.085	-17.80	-4.66	0.950	-0.085	-17.80	-4.66	0.950	-0.085	-17.80	-4.66	0.950	-0.085	-17.80	-4.66	0.950	-0.085
-18.60	-4.81	0.994	-0.089	-18.60	-4.81	0.994	-0.089	-18.60	-4.81	0.994	-0.089	-18.60	-4.81	0.994	-0.089	-18.60	-4.81	0.994	-0.089
-19.40	-4.96	1.038	-0.093	-19.40	-4.96	1.038	-0.093	-19.40	-4.96	1.038	-0.093	-19.40	-4.96	1.038	-0.093	-19.40	-4.96	1.038	-0.093
-20.20	-5.11	1.082	-0.097	-20.20	-5.11	1.082	-0.097	-20.20	-5.11	1.082	-0.097	-20.20	-5.11	1.082	-0.097	-20.20	-5.11	1.082	-0.097
-21.00	-5.26	1.126	-0.101	-21.00	-5.26	1.126	-0.101	-21.00	-5.26	1.126	-0.101	-21.00	-5.26	1.126	-0.101	-21.00	-5.26	1.126	-0.101
-21.80	-5.41	1.170	-0.105	-21.80	-5.41	1.170	-0.105	-21.80	-5.41	1.170	-0.105	-21.80	-5.41	1.170	-0.105	-21.80	-5.41	1.170	-0.105
-22.60	-5.56	1.214	-0.109	-22.60	-5.56	1.214	-0.109	-22.60	-5.56	1.214	-0.109	-22.60	-5.56	1.214	-0.109	-22.60	-5.56	1.214	-0.109
-23.40	-5.71	1.258	-0.113	-23.40	-5.71	1.258	-0.113	-23.40	-5.71	1.258	-0.113	-23.40	-5.71	1.258	-0.113	-23.40	-5.71	1.258	-0.113
-24.20	-5.86	1.302	-0.117	-24.20	-5.86	1.302	-0.117	-24.20	-5.86	1.302	-0.117	-24.20	-5.86	1.302	-0.117	-24.20	-5.86	1.302	-0.117
-25.00	-6.01	1.346	-0.121	-25.00	-6.01	1.346	-0.121	-25.00	-6.01	1.346	-0.121	-25.00	-6.01	1.346	-0.121	-25.00	-6.01	1.346	-0.121
-25.80	-6.16	1.390	-0.125	-25.80	-6.16	1.390	-0.125	-25.80	-6.16	1.390	-0.125	-25.80	-6.16	1.390	-0.125	-25.80	-6.16	1.390	-0.125
-26.60	-6.31	1.434	-0.129	-26.60	-6.31	1.434	-0.129	-26.60	-6.31	1.434	-0.129	-26.60	-6.31	1.434	-0.129	-26.60	-6.31	1.434	-0.129
-27.40	-6.46	1.478	-0.133	-27.40	-6.46	1.478	-0.133	-27.40	-6.46	1.478	-0.133	-27.40	-6.46	1.478	-0.133	-27.40	-6.46	1.478	-0.133
-28.20	-6.61	1.522	-0.137	-28.20	-6.61	1.522	-0.137	-28.20	-6.61	1.522	-0.137	-28.20	-6.61	1.522	-0.137	-28.20	-6.61	1.522	-0.137
-29.00	-6.76	1.566	-0.141	-29.00	-6.76	1.566	-0.141	-29.00	-6.76	1.566	-0.141	-29.00	-6.76	1.566	-0.141	-29.00	-6.76	1.566	-0.141
-29.80	-6.91	1.610	-0.145	-29.80	-6.91	1.610	-0.145	-29.80	-6.91	1.610	-0.145	-29.80	-6.91	1.610	-0.145	-29.80	-6.91	1.610	-0.145
-30.60	-7.06	1.654	-0.149	-30.60	-7.06	1.654	-0.149	-30.60	-7.06	1.654	-0.149	-30.60	-7.06	1.654	-0.149	-30.60	-7.06	1.654	-0.149
-31.40	-7.21	1.698	-0.153	-31.40	-7.21	1.698	-0.153	-31.40	-7.21	1.698	-0.153	-31.40	-7.21	1.698	-0.153	-31.40	-7.21	1.698	-0.153
-32.20	-7.36	1.742	-0.157	-32.20	-7.36	1.742	-0.157	-32.20	-7.36	1.742	-0.157	-32.20	-7.36	1.742	-0.157	-32.20	-7.36	1.742	-0.157
-33.00	-7.51	1.786	-0.161	-33.00	-7.51	1.786	-0.161	-33.00	-7.51	1.786	-0.161	-33.00	-7.51	1.786	-0.161	-33.00	-7.51	1.786	-0.161
-33.80	-7.66	1.830	-0.165	-33.80	-7.66	1.830	-0.165	-33.80	-7.66	1.830	-0.165	-33.80	-7.66	1.830	-0.165	-33.80	-7.66	1.830	-0.165
-34.60	-7.81	1.874	-0.169	-34.60	-7.81	1.874	-0.169	-34.60	-7.81	1.874	-0.169	-34.60	-7.81	1.874	-0.169	-34.60	-7.81	1.874	-0.169
-35.40	-7.96	1.918	-0.173	-35.40	-7.96	1.918	-0.173	-35.40	-7.96	1.918	-0.173	-35.40	-7.96	1.918	-0.173	-35.40	-7.96	1.918	-0.173
-36.20	-8.11	1.962	-0.177	-36.20	-8.11	1.962	-0.177	-36.20	-8.11	1.962	-0.177	-36.20	-8.11	1.962	-0.177	-36.20	-8.11	1.962	-0.177
-37.00	-8.26	2.006	-0.181	-37.00	-8.26	2.006	-0.181	-37.00	-8.26	2.006	-0.181	-37.00	-8.26	2.006	-0.181	-37.00	-8.26	2.006	-0.181
-37.80	-8.41	2.050	-0.185	-37.80	-8.41	2.050	-0.185	-37.80	-8.41	2.050	-0.185	-37.80	-8.41	2.050	-0.185	-37.80	-8.41	2.050	-0.185
-38.60	-8.56	2.094	-0.189	-38.60	-8.56	2.094	-0.189	-38.60	-8.56	2.094	-0.189	-38.60	-8.56	2.094	-0.189	-38.60	-8.56	2.094	-0.189
-39.40	-8.71	2.138	-0.193	-39.40	-8.71	2.138	-0.193	-39.40	-8.71	2.138	-0.193	-39.40	-8.71	2.138	-0.193	-39.40	-8.71	2.138	-0.193
-40.20	-8.86	2.182	-0.197	-40.20	-8.86	2.182	-0.197	-40.20	-8.86	2.182	-0.197	-40.20	-8.86	2.182	-0.197	-40.20	-8.86	2.182	-0.197
-41.00	-9.01	2.226	-0.201	-41.00	-9.01	2.226	-0.201	-41.00	-9.01	2.226	-0.201	-41.00	-9.01	2.226	-0.201	-41.00	-9.01	2.226	-0.201
-41.80	-9.16	2.270	-0.205	-41.80	-9.16	2.270	-0.205	-41.80	-9.16	2.270	-0.205	-41.80	-9.16	2.270	-0.205	-41.80	-9.16	2.270	-0.205
-42.60	-9.31	2.314	-0.209	-42.60	-9														

TABLE II.- AERODYNAMIC CHARACTERISTICS OF THE RECTANGULAR  
WING WITH 3-PERCENT-THICK ROUNDED-NOSE SECTION

$\alpha$	$C_L$	$C_D$	$C_M$	$\alpha$	$C_L$	$C_D$	$C_M$	$\alpha$	$C_L$	$C_D$	$C_M$	$\alpha$	$C_L$	$C_D$	$C_M$	$\alpha$	$C_L$	$C_D$	$C_M$	$\alpha$	$C_L$	$C_D$	$C_M$
M=0.61 R=1.8x10 <sup>6</sup>				M=0.71 R=1.8x10 <sup>6</sup>				M=0.81 R=1.8x10 <sup>6</sup>				M=0.91 R=1.8x10 <sup>6</sup>				M=0.93 R=1.8x10 <sup>6</sup>				M=1.20 R=1.8x10 <sup>6</sup>			
-0.87	-0.086	0.0072	0	-0.86	-0.087	0.0079	0	-0.80	-0.031	0.0076	0.001	-0.88	-0.028	0.0072	-0.004	-0.29	-0.066	0.0071	-0.004	-0.29	-0.026	0.0171	0.008
-0.95	-0.040	0.0076	-0.002	-0.95	-0.041	0.0078	-0.002	-0.96	-0.044	0.0077	-0.002	-0.96	-0.036	0.0074	-0.007	-0.96	-0.030	0.0074	-0.008	-0.94	-0.045	0.0161	0.003
-0.82	-0.054	0.0079	-0.003	-0.82	-0.056	0.0079	-0.004	-0.82	-0.058	0.0079	-0.004	-0.83	-0.045	0.0077	-0.011	-0.83	-0.050	0.0080	-0.013	-0.81	-0.062	0.0158	0.004
-1.07	-0.062	0.0082	-0.005	-1.07	-0.060	0.0080	-0.005	-1.11	-0.070	0.0082	-0.007	-0.79	-0.060	0.0085	-0.012	-1.00	-0.061	0.0082	-0.016	-1.08	-0.079	0.0178	0.004
-2.13	-0.118	0.0096	-0.010	-2.17	-0.122	0.0096	-0.011	-2.20	-0.127	0.0119	-0.014	-2.20	-0.128	0.0107	-0.014	-2.21	-0.128	0.0107	-0.016	-2.16	-0.148	0.0174	0.010
-3.23	-0.178	0.0138	-0.013	-3.27	-0.182	0.0140	-0.016	-3.28	-0.182	0.0140	-0.016	-3.30	-0.183	0.0131	-0.013	-3.32	-0.180	0.0130	-0.016	-3.21	-0.209	0.0171	0.016
-4.30	-0.233	0.0202	-0.017	-4.33	-0.236	0.0209	-0.020	-4.36	-0.239	0.0221	-0.026	-4.41	-0.240	0.0217	-0.033	-4.42	-0.242	0.0215	-0.027	-4.29	-0.268	0.0274	0.020
-5.39	-0.290	0.0271	-0.024	-5.42	-0.293	0.0278	-0.027	-5.45	-0.296	0.0290	-0.034	-5.48	-0.299	0.0286	-0.041	-5.50	-0.302	0.0284	-0.045	-5.43	-0.328	0.0321	0.024
-6.48	-0.348	0.0341	-0.034	-6.51	-0.351	0.0348	-0.037	-6.54	-0.354	0.0360	-0.044	-6.57	-0.357	0.0356	-0.051	-6.60	-0.360	0.0354	-0.055	-6.53	-0.384	0.0388	0.028
-7.57	-0.403	0.0410	-0.043	-7.60	-0.406	0.0417	-0.046	-7.63	-0.409	0.0429	-0.054	-7.66	-0.412	0.0425	-0.061	-7.69	-0.415	0.0423	-0.065	-7.62	-0.438	0.0452	0.032
-8.66	-0.458	0.0479	-0.051	-8.69	-0.461	0.0486	-0.054	-8.72	-0.464	0.0498	-0.062	-8.75	-0.467	0.0494	-0.069	-8.78	-0.470	0.0492	-0.073	-8.71	-0.491	0.0511	0.036
-9.75	-0.513	0.0548	-0.060	-9.78	-0.516	0.0555	-0.063	-9.81	-0.519	0.0567	-0.070	-9.84	-0.522	0.0563	-0.077	-9.87	-0.525	0.0561	-0.081	-9.80	-0.544	0.0530	0.040
-10.84	-0.568	0.0617	-0.067	-10.87	-0.571	0.0624	-0.070	-10.90	-0.574	0.0636	-0.077	-10.93	-0.577	0.0632	-0.084	-10.96	-0.580	0.0630	-0.088	-10.89	-0.600	0.0549	0.044
-11.93	-0.623	0.0686	-0.074	-11.96	-0.626	0.0693	-0.077	-11.99	-0.629	0.0705	-0.084	-12.02	-0.632	0.0701	-0.091	-12.05	-0.635	0.0699	-0.095	-11.98	-0.654	0.0568	0.048
-13.02	-0.678	0.0755	-0.081	-13.05	-0.681	0.0762	-0.084	-13.08	-0.684	0.0774	-0.091	-13.11	-0.687	0.0770	-0.098	-13.14	-0.690	0.0768	-0.102	-13.07	-0.671	0.0587	0.052
-14.11	-0.733	0.0824	-0.090	-14.14	-0.736	0.0831	-0.093	-14.17	-0.739	0.0843	-0.100	-14.20	-0.742	0.0839	-0.107	-14.23	-0.745	0.0837	-0.111	-14.16	-0.722	0.0606	0.056
-15.20	-0.788	0.0893	-0.097	-15.23	-0.791	0.0900	-0.100	-15.26	-0.794	0.0912	-0.107	-15.29	-0.797	0.0908	-0.114	-15.32	-0.800	0.0906	-0.118	-15.25	-0.779	0.0625	0.060
-16.29	-0.843	0.0962	-0.104	-16.32	-0.846	0.0969	-0.107	-16.35	-0.849	0.0981	-0.114	-16.38	-0.852	0.0977	-0.121	-16.41	-0.855	0.0975	-0.125	-16.34	-0.836	0.0644	0.064
-17.38	-0.898	0.1031	-0.111	-17.41	-0.901	0.1038	-0.114	-17.44	-0.904	0.1050	-0.121	-17.47	-0.907	0.1046	-0.128	-17.50	-0.910	0.1044	-0.132	-17.43	-0.890	0.0663	0.068
-18.47	-0.953	0.1100	-0.118	-18.50	-0.956	0.1107	-0.121	-18.53	-0.959	0.1119	-0.128	-18.56	-0.962	0.1115	-0.135	-18.59	-0.965	0.1113	-0.139	-18.52	-0.946	0.0682	0.072
-19.56	-1.008	0.1169	-0.125	-19.59	-1.011	0.1176	-0.128	-19.62	-1.014	0.1188	-0.135	-19.65	-1.017	0.1184	-0.142	-19.68	-1.020	0.1182	-0.146	-19.61	-1.001	0.0701	0.076
-20.65	-1.063	0.1238	-0.132	-20.68	-1.066	0.1245	-0.135	-20.71	-1.069	0.1257	-0.142	-20.74	-1.072	0.1253	-0.149	-20.77	-1.075	0.1251	-0.153	-20.70	-1.056	0.0720	0.080
-21.74	-1.118	0.1307	-0.139	-21.77	-1.121	0.1314	-0.142	-21.80	-1.124	0.1326	-0.149	-21.83	-1.127	0.1322	-0.156	-21.86	-1.130	0.1320	-0.160	-21.79	-1.113	0.0739	0.084
-22.83	-1.173	0.1376	-0.146	-22.86	-1.176	0.1383	-0.149	-22.89	-1.179	0.1395	-0.156	-22.92	-1.182	0.1391	-0.163	-22.95	-1.185	0.1389	-0.167	-22.88	-1.168	0.0758	0.088
-23.92	-1.228	0.1445	-0.153	-23.95	-1.231	0.1452	-0.156	-23.98	-1.234	0.1464	-0.163	-24.01	-1.237	0.1460	-0.170	-24.04	-1.240	0.1458	-0.174	-23.97	-1.223	0.0777	0.092
-25.01	-1.283	0.1514	-0.160	-25.04	-1.286	0.1521	-0.163	-25.07	-1.289	0.1533	-0.170	-25.10	-1.292	0.1529	-0.177	-25.13	-1.295	0.1527	-0.181	-25.06	-1.276	0.0796	0.096
-26.10	-1.338	0.1583	-0.167	-26.13	-1.341	0.1590	-0.170	-26.16	-1.344	0.1602	-0.177	-26.19	-1.347	0.1598	-0.184	-26.22	-1.350	0.1596	-0.188	-26.15	-1.333	0.0815	0.100
-27.19	-1.393	0.1652	-0.174	-27.22	-1.396	0.1659	-0.177	-27.25	-1.399	0.1671	-0.184	-27.28	-1.402	0.1667	-0.191	-27.31	-1.405	0.1665	-0.195	-27.24	-1.386	0.0834	0.104
-28.28	-1.448	0.1721	-0.181	-28.31	-1.451	0.1728	-0.184	-28.34	-1.454	0.1740	-0.191	-28.37	-1.457	0.1736	-0.198	-28.40	-1.460	0.1734	-0.202	-28.33	-1.443	0.0853	0.108
-29.37	-1.503	0.1790	-0.188	-29.40	-1.506	0.1797	-0.191	-29.43	-1.509	0.1809	-0.198	-29.46	-1.512	0.1805	-0.205	-29.49	-1.515	0.1803	-0.209	-29.42	-1.496	0.0872	0.112
-30.46	-1.558	0.1859	-0.195	-30.49	-1.561	0.1866	-0.202	-30.52	-1.564	0.1878	-0.209	-30.55	-1.567	0.1874	-0.216	-30.58	-1.570	0.1872	-0.220	-30.51	-1.553	0.0891	0.116
-31.55	-1.613	0.1928	-0.202	-31.58	-1.616	0.1935	-0.209	-31.61	-1.619	0.1947	-0.216	-31.64	-1.622	0.1943	-0.223	-31.67	-1.625	0.1941	-0.227	-31.60	-1.606	0.0910	0.120
-32.64	-1.668	0.1997	-0.209	-32.67	-1.671	0.2004	-0.216	-32.70	-1.674	0.2016	-0.223	-32.73	-1.677	0.2012	-0.230	-32.76	-1.680	0.2010	-0.234	-32.69	-1.663	0.0929	0.124
-33.73	-1.723	0.2066	-0.216	-33.76	-1.726	0.2073	-0.223	-33.79	-1.729	0.2085	-0.230	-33.82	-1.732	0.2081	-0.237	-33.85	-1.735	0.2079	-0.241	-33.78	-1.718	0.0948	0.128
-34.82	-1.778	0.2135	-0.223	-34.85	-1.781	0.2142	-0.230	-34.88	-1.784	0.2154	-0.237	-34.91	-1.787	0.2150	-0.244	-34.94	-1.790	0.2148	-0.248	-34.87	-1.773	0.0967	0.132
-35.91	-1.833	0.2204	-0.230	-35.94	-1.836	0.2211	-0.237	-35.97	-1.839	0.2223	-0.244	-36.00	-1.842	0.2219	-0.251	-36.03	-1.845	0.2217	-0.255	-35.96	-1.828	0.0986	0.136
-37.00	-1.888	0.2273	-0.237	-37.03	-1.891	0.2278	-0.244	-37.06	-1.894	0.2290	-0.251	-37.09	-1.897	0.2286	-0.258	-37.12	-1.900	0.2284	-0.262	-37.05	-1.883	0.1005	0.140
-38.09	-1.943	0.2342	-0.244	-38.12	-1.946	0.2349	-0.251	-38.15	-1.949	0.2361	-0.258	-38.18	-1.952	0.2357	-0.265	-38.21	-1.955	0.2355	-0.269	-38.14	-1.938	0.1024	0.144
-39.18	-1.998	0.2411	-0.251	-39.21	-2.001	0.2418	-0.258	-39.24	-2.004	0.2430	-0.265	-39.27	-2.007	0.2426	-0.272	-39.30	-2.010	0.2424	-0.276	-39.23	-1.993	0.1043	0.148
-40.27	-2.053	0.2480	-0.258	-40.30	-2.056	0.2487	-0.265	-40.33	-2.059	0.2499	-0.272	-40.36	-2.062	0.2495	-0.279	-40.39	-2.065	0.2493	-0.283	-40.32	-2.048	0.1062	0.152
-41.36	-2.108	0.2549	-0.265	-41.39	-2.111	0.2556	-0.272	-41.42	-2.114	0.2568	-0.279	-41.45	-2.117	0.2564	-0.286	-41.48	-2.120	0.2562	-0.290	-41.41	-2.103	0.1081	0.156
-42.45	-2.163	0.2618	-0.272	-42.48	-2.166	0.2625	-0.279	-42.51	-2.169	0.2637	-0.286	-42.54	-2.172	0.2633	-0.293	-42.57	-2.175	0.2631	-0.297	-42.50	-2.158	0.1100	0.160
-43.54	-2.218	0.2687	-0.279	-43.57	-2.221	0.2694	-0.286	-43.60	-2.224	0.2706	-0.293	-43.63	-2.227	0.2702	-0.300	-43.66	-2.230	0.2700	-0.304	-43.59	-2.213	0.1119	0.164
-44.63	-2.273	0.2756	-0.286	-44.66	-2.276	0.2763	-0.293	-44.69	-2.279	0.2775	-0.300	-44.72	-2.282	0.2771	-0.307	-44.75	-2.285	0.2769	-0.311	-444.6			



TABLE IV.- AERODYNAMIC CHARACTERISTICS OF THE SWEEPED-BACK WING WITH 3-PERCENT-THICK ROUNDED-NOSE SECTION

N=0.61 R=1.9x10 <sup>10</sup>				N=0.71 R=1.9x10 <sup>10</sup>				N=0.81 R=1.9x10 <sup>10</sup>				N=0.91 R=1.9x10 <sup>10</sup>				N=0.93 R=1.9x10 <sup>10</sup>				N=1.00 R=1.9x10 <sup>10</sup>			
a	c <sub>L</sub>	c <sub>D</sub>	c <sub>m</sub>	a	c <sub>L</sub>	c <sub>D</sub>	c <sub>m</sub>	a	c <sub>L</sub>	c <sub>D</sub>	c <sub>m</sub>	a	c <sub>L</sub>	c <sub>D</sub>	c <sub>m</sub>	a	c <sub>L</sub>	c <sub>D</sub>	c <sub>m</sub>	a	c <sub>L</sub>	c <sub>D</sub>	c <sub>m</sub>
-0.27	-0.023	0.0078	-0.001	-0.25	-0.023	0.0073	0	-0.26	-0.023	0.0062	-0.001	-0.26	-0.022	0.0071	-0.002	-0.27	-0.023	0.0079	-0.002	-0.28	-0.023	0.0109	0.000
-0.24	-0.039	0.0080	-0.001	-0.24	-0.039	0.0084	0	-0.24	-0.039	0.0081	-0.002	-0.25	-0.032	0.0080	-0.004	-0.25	-0.039	0.0080	-0.002	-0.23	-0.043	0.0115	0.000
-0.21	-0.048	0.0089	-0.002	-0.21	-0.049	0.0097	-0.002	-0.22	-0.046	0.0093	-0.002	-0.21	-0.044	0.0089	-0.005	-0.21	-0.044	0.0090	-0.006	-0.20	-0.050	0.0123	0.000
-0.17	-0.058	0.0094	-0.002	-0.18	-0.059	0.0097	-0.002	-0.18	-0.059	0.0093	-0.003	-0.18	-0.057	0.0089	-0.007	-0.18	-0.056	0.0096	-0.007	-0.16	-0.062	0.0132	0.010
-0.13	-0.112	0.0116	-0.01	-0.13	-0.116	0.012	-0.01	-0.13	-0.116	0.0119	-0.01	-0.13	-0.112	0.011	-0.01	-0.13	-0.112	0.011	-0.01	-0.13	-0.112	0.012	0.010
-0.19	-0.169	0.0131	0	-0.20	-0.175	0.0166	0.001	-0.20	-0.179	0.0169	0.001	-0.20	-0.188	0.0177	-0.002	-0.20	-0.187	0.0176	-0.007	-0.15	-0.184	0.0132	0.010
-0.26	-0.230	0.021	0.005	-0.24	-0.239	0.024	0.006	-0.24	-0.249	0.027	0.006	-0.24	-0.260	0.026	0.004	-0.24	-0.273	0.027	0.004	-0.23	-0.273	0.0316	0.010
0.25	0.002	0.0059	0	0.25	-0.001	0.0073	0	0.25	0.002	0.0059	-0.001	0.25	0.004	0.0070	-0.001	0.25	0.005	0.0062	-0.001	0.25	0	0.0113	0
0.21	0.014	0.0070	-0.003	0.22	0.017	0.0076	-0.001	0.23	0.019	0.0073	-0.001	0.23	0.022	0.0069	-0.001	0.23	0.021	0.0074	-0.001	0.24	0.016	0.0113	0
0.17	0.025	0.0073	0	0.18	0.029	0.0074	0	0.19	0.032	0.0071	-0.001	0.19	0.036	0.0070	-0.001	0.19	0.035	0.0075	-0.001	0.18	0.034	0.0117	-0.001
1.04	0.038	0.0076	0	1.06	0.043	0.0089	0	1.05	0.045	0.0091	0	1.05	0.047	0.0091	0	1.07	0.049	0.0092	0	1.07	0.049	0.0121	0
0.71	0.091	0.0085	-0.002	0.73	0.101	0.0106	-0.001	0.74	0.102	0.0112	-0.001	0.75	0.108	0.0111	0	0.75	0.108	0.011	0	0.75	0.108	0.0116	0.010
0.37	0.145	0.0143	-0.002	0.38	0.157	0.0149	-0.005	0.39	0.165	0.0151	-0.005	0.39	0.176	0.0159	-0.003	0.39	0.177	0.0168	-0.002	0.39	0.177	0.0214	0.010
0.23	0.204	0.0206	-0.003	0.27	0.221	0.0215	-0.004	0.29	0.232	0.0231	-0.006	0.31	0.249	0.0234	-0.006	0.32	0.254	0.0248	-0.009	0.32	0.254	0.0248	0.010
0.37	0.335	0.0406	-0.007	0.42	0.353	0.0428	-0.010	0.43	0.366	0.0446	-0.013	0.45	0.381	0.0458	-0.016	0.46	0.391	0.0471	-0.019	0.47	0.391	0.0471	0.010
0.43	0.466	0.0566	-0.012	0.48	0.473	0.0579	-0.013	0.48	0.479	0.0586	-0.016	0.49	0.486	0.0593	-0.019	0.50	0.493	0.0600	-0.022	0.50	0.493	0.0600	0.010
0.50	0.538	0.0665	-0.015	0.53	0.545	0.0679	-0.018	0.54	0.552	0.0686	-0.021	0.55	0.560	0.0693	-0.024	0.56	0.567	0.0700	-0.027	0.56	0.567	0.0700	0.010
0.58	0.610	0.0764	-0.018	0.61	0.617	0.0779	-0.021	0.62	0.624	0.0786	-0.024	0.63	0.632	0.0793	-0.027	0.64	0.639	0.0800	-0.030	0.64	0.639	0.0800	0.010
0.66	0.682	0.0863	-0.021	0.69	0.689	0.0879	-0.024	0.70	0.696	0.0886	-0.027	0.71	0.704	0.0893	-0.030	0.72	0.711	0.0900	-0.033	0.72	0.711	0.0900	0.010
0.74	0.704	0.0962	-0.024	0.77	0.711	0.0989	-0.027	0.78	0.718	0.0996	-0.030	0.79	0.726	0.1003	-0.033	0.80	0.733	0.1010	-0.036	0.80	0.733	0.1010	0.010
0.82	0.814	0.1061	-0.027	0.85	0.821	0.1089	-0.030	0.86	0.828	0.1096	-0.033	0.87	0.836	0.1103	-0.036	0.88	0.843	0.1110	-0.039	0.88	0.843	0.1110	0.010
0.90	0.896	0.1160	-0.030	0.93	0.903	0.1217	-0.033	0.94	0.910	0.1224	-0.036	0.95	0.918	0.1231	-0.039	0.96	0.925	0.1238	-0.042	0.96	0.925	0.1238	0.010
0.98	0.978	0.1316	-0.033	1.00	0.985	0.1365	-0.036	1.00	0.992	0.1414	-0.039	1.00	0.999	0.1463	-0.042	1.00	1.006	0.1512	-0.045	1.00	1.006	0.1512	0.010
-0.27	-0.023	0.0078	-0.001	-0.25	-0.023	0.0073	0	-0.26	-0.023	0.0062	-0.001	-0.26	-0.022	0.0071	-0.002	-0.27	-0.023	0.0079	-0.002	-0.28	-0.023	0.0109	0.000
-0.24	-0.039	0.0080	-0.001	-0.24	-0.039	0.0084	0	-0.24	-0.039	0.0081	-0.002	-0.25	-0.032	0.0080	-0.004	-0.25	-0.039	0.0080	-0.002	-0.23	-0.043	0.0115	0.000
-0.21	-0.048	0.0089	-0.002	-0.21	-0.049	0.0097	-0.002	-0.22	-0.046	0.0093	-0.002	-0.21	-0.044	0.0089	-0.005	-0.21	-0.044	0.0090	-0.006	-0.20	-0.050	0.0123	0.000
-0.17	-0.058	0.0094	-0.002	-0.18	-0.059	0.0097	-0.002	-0.18	-0.059	0.0093	-0.003	-0.18	-0.057	0.0089	-0.007	-0.18	-0.056	0.0096	-0.007	-0.16	-0.062	0.0132	0.010
-0.13	-0.112	0.0116	-0.01	-0.13	-0.116	0.012	-0.01	-0.13	-0.116	0.0119	-0.01	-0.13	-0.112	0.011	-0.01	-0.13	-0.112	0.011	-0.01	-0.13	-0.112	0.012	0.010
-0.19	-0.169	0.0131	0	-0.20	-0.175	0.0166	0.001	-0.20	-0.179	0.0169	0.001	-0.20	-0.188	0.0177	-0.002	-0.20	-0.187	0.0176	-0.007	-0.15	-0.184	0.0132	0.010
-0.26	-0.230	0.021	0.005	-0.24	-0.239	0.024	0.006	-0.24	-0.249	0.027	0.006	-0.24	-0.260	0.026	0.004	-0.24	-0.273	0.027	0.004	-0.23	-0.273	0.0316	0.010
0.25	0.002	0.0059	0	0.25	-0.001	0.0073	0	0.25	0.002	0.0059	-0.001	0.25	0.004	0.0070	-0.001	0.25	0.005	0.0062	-0.001	0.25	0	0.0113	0
0.21	0.014	0.0070	-0.003	0.22	0.017	0.0076	-0.001	0.23	0.019	0.0073	-0.001	0.23	0.022	0.0069	-0.001	0.23	0.021	0.0074	-0.001	0.24	0.016	0.0113	0
0.17	0.025	0.0073	0	0.18	0.029	0.0074	0	0.19	0.032	0.0071	-0.001	0.19	0.036	0.0070	-0.001	0.19	0.035	0.0075	-0.001	0.18	0.034	0.0117	-0.001
1.04	0.038	0.0076	0	1.06	0.043	0.0089	0	1.05	0.045	0.0091	0	1.05	0.047	0.0091	0	1.07	0.049	0.0092	0	1.07	0.049	0.0121	0
0.71	0.091	0.0085	-0.002	0.73	0.101	0.0106	-0.001	0.74	0.102	0.0112	-0.001	0.75	0.108	0.0111	0	0.75	0.108	0.011	0	0.75	0.108	0.0116	0.010
0.37	0.145	0.0143	-0.002	0.38	0.157	0.0149	-0.005	0.39	0.165	0.0151	-0.005	0.39	0.176	0.0159	-0.003	0.39	0.177	0.0168	-0.002	0.39	0.177	0.0214	0.010
0.23	0.204	0.0206	-0.003	0.27	0.221	0.0215	-0.004	0.29	0.232	0.0231	-0.006	0.31	0.249	0.0234	-0.006	0.32	0.254	0.0248	-0.009	0.32	0.254	0.0248	0.010
0.37	0.335	0.0406	-0.007	0.42	0.353	0.0428	-0.010	0.43	0.366	0.0446	-0.013	0.45	0.381	0.0458	-0.016	0.46	0.391	0.0471	-0.019	0.47	0.391	0.0471	0.010
0.43	0.466	0.0566	-0.012	0.48	0.473	0.0579	-0.013	0.48	0.479	0.0586	-0.016	0.49	0.486	0.0593	-0.019	0.50	0.493	0.0600	-0.022	0.50	0.493	0.0600	0.010
0.50	0.538	0.0665	-0.015	0.53	0.545	0.0679	-0.018	0.54	0.552	0.0686	-0.021	0.55	0.560	0.0693	-0.024	0.56	0.567	0.0700	-0.027	0.56	0.567	0.0700	0.010
0.58	0.610	0.0764	-0.018	0.61	0.617	0.0779	-0.021	0.62	0.624	0.0786	-0.024	0.63	0.632	0.0793	-0.027	0.64	0.639	0.0800	-0.030	0.64	0.639	0.0800	0.010
0.66	0.682	0.0863	-0.021	0.69	0.689	0.0879	-0.024	0.70	0.696	0.0886	-0.027	0.71	0.704	0.0893	-0.030	0.72	0.711	0.0900	-0.033	0.72	0.711	0.0900	0.010
0.74	0.704	0.0962	-0.024	0.77	0.711	0.0989	-0.027	0.78	0.718	0.0996	-0.030	0.79	0.726	0.1003	-0.033	0.80	0.733	0.1010	-0.036	0.80	0.733	0.1010	0.010
0.82	0.814	0.1061	-0.027	0.85	0.821	0.1089	-0.030	0.86	0.828	0.1096	-0.033	0.87	0.836	0.1103	-0.036	0.88	0.843	0.1110	-0.039	0.88	0.843	0.1110	0.010
0.90	0.896	0.1160	-0.030	0.93	0.903	0.1217	-0.033	0.94	0.910	0.1224	-0.036	0.95	0.918	0.1231	-0.039	0.96	0.925	0.1238	-0.042	0.96	0.925	0.1238	0.010
0.98	0.978	0.1316	-0.033	1.00	0.985	0.1365	-0.036	1.00	0.992	0.1414	-0.039	1.00	0.999	0.1463	-0.042	1.00	1.006	0.1512	-0.045	1.00	1.006	0.1512	0.010
-0.27	-0.023	0.0078	-0.001	-0.25	-0.023	0.0073	0	-0.26	-0.023	0.0062	-0.001	-0.26	-0.022	0.0071	-0.002	-0.27	-0.023	0.0079	-0.002	-0.28	-0.023	0.0109	0.000
-0.24	-0.039	0.0080	-0.001	-0.24	-0.039	0.0084	0	-0.24	-0.039	0.0081	-0.002	-0.25	-0.032	0.0080	-0.004	-0.25	-0.039	0.0080	-0.002	-0.23	-0.043	0.0115	0.000
-0.21	-0.048	0.0089	-0.002	-0.21	-0.049	0.0097	-0.002	-0.22	-0.046	0.0093	-0.002	-0.21	-0.044	0.0089	-0.005	-0.21	-0.044	0.0090	-0.006	-0.20	-0.050	0.0123	0.000
-0.17	-0.058	0.0094	-0.002	-0.18	-0.059	0.0097	-0.002	-0.18	-0.059	0.0093	-0.003	-0.18	-0.057	0.0089	-0.007	-0.18	-0.056	0.0096	-0.007	-0.16	-0.0		

TABLE V.- AERODYNAMIC CHARACTERISTICS OF THE TRIANGULAR  
WING OF REFERENCE 1

$\alpha$	$C_L$	$C_D$	$C_M$	$\alpha$	$C_L$	$C_D$	$C_M$	$\alpha$	$C_L$	$C_D$	$C_M$	$\alpha$	$C_L$	$C_D$	$C_M$	$\alpha$	$C_L$	$C_D$	$C_M$	$\alpha$	$C_L$	$C_D$	$C_M$	$\alpha$	$C_L$	$C_D$	$C_M$	$\alpha$	$C_L$	$C_D$	$C_M$	
M=0.61 B=3.0x10°				M=0.81 B=3.0x10°				M=0.91 B=3.0x10°				M=1.30 B=3.0x10°				M=1.40 B=3.0x10°				M=1.53 B=3.0x10°				M=1.60 B=3.0x10°				M=1.70 B=3.0x10°				
0	0	0.0070	-0.003	0	-0.003	0.0067	-0.003	0	0.001	0.0074	-0.004	0	-0.003	0.0092	-0.001	0	-0.002	0.0104	-0.001	-0.01	-0.006	0.0103	0	0	-0.003	0.0088	-0.001	0	-0.003	0.0097	-0.003	0
-6.43	-0.266	0.361	-0.035	-6.51	-0.325	0.418	-0.028	-6.97	-0.356	0.487	-0.069	-6.19	-0.290	0.399	-0.073	-6.19	-0.266	0.399	-0.071	-6.18	-0.260	0.373	-0.069	-6.43	-0.266	0.361	-0.035	-6.51	-0.325	0.418	-0.028	
-7.36	-0.240	0.270	-0.034	-7.42	-0.263	0.297	-0.041	-7.45	-0.261	0.222	-0.021	-7.15	-0.243	0.300	-0.061	-7.16	-0.236	0.305	-0.060	-7.15	-0.229	0.293	-0.029	-7.36	-0.240	0.270	-0.034	-7.42	-0.263	0.297	-0.041	
-8.26	-0.187	0.190	-0.026	-8.32	-0.203	0.203	-0.031	-8.35	-0.221	0.089	-0.039	-8.13	-0.193	0.229	-0.048	-8.14	-0.186	0.229	-0.047	-8.13	-0.176	0.205	-0.024	-8.26	-0.187	0.190	-0.026	-8.32	-0.203	0.203	-0.031	
-9.20	-0.137	0.132	-0.018	-9.23	-0.150	0.142	-0.023	-9.26	-0.162	0.036	-0.025	-9.03	-0.142	0.168	-0.039	-9.04	-0.139	0.176	-0.034	-9.03	-0.130	0.171	-0.022	-9.20	-0.137	0.132	-0.018	-9.23	-0.150	0.142	-0.023	
-10.14	-0.091	0.097	-0.011	-10.16	-0.097	0.101	-0.013	-10.18	-0.102	0.016	-0.006	-9.95	-0.095	0.129	-0.022	-9.96	-0.093	0.136	-0.022	-9.95	-0.087	0.133	-0.021	-10.14	-0.091	0.097	-0.011	-10.16	-0.097	0.101	-0.013	
-11.08	-0.048	0.078	-0.004	-11.08	-0.090	0.073	-0.005	-11.05	-0.092	0.083	-0.006	-11.03	-0.047	0.102	-0.010	-11.03	-0.049	0.113	-0.010	-11.03	-0.045	0.107	-0.010	-11.08	-0.048	0.078	-0.004	-11.08	-0.090	0.073	-0.005	
0	0.004	0.007	-0.002	0	-0.004	0.0068	-0.003	0	-0.004	0.0075	-0.003	0	-0.003	0.0094	-0.001	0	-0.005	0.0104	-0.001	0	-0.005	0.0096	0	0	-0.004	0.007	-0.002	0	-0.004	0.0068	-0.003	0
1.06	0.044	0.024	-0.010	1.07	0.048	0.028	-0.011	1.08	0.051	0.037	-0.012	1.03	0.041	0.039	-0.012	1.03	0.044	0.044	-0.013	1.03	0.044	0.044	-0.013	1.06	0.044	0.024	-0.010	1.07	0.048	0.028	-0.011	
2.12	0.066	0.029	-0.017	2.15	0.100	0.010	-0.020	2.17	0.103	0.022	-0.022	2.06	0.087	0.031	-0.024	2.06	0.089	0.040	-0.025	2.06	0.087	0.036	-0.024	2.12	0.066	0.029	-0.017	2.15	0.100	0.010	-0.020	
3.19	0.134	0.137	-0.023	3.23	0.189	0.017	-0.029	3.25	0.164	0.069	-0.035	3.09	0.135	0.070	-0.037	3.09	0.132	0.078	-0.037	3.09	0.129	0.077	-0.036	3.19	0.134	0.137	-0.023	3.23	0.189	0.017	-0.029	
4.26	0.193	0.202	-0.031	4.31	0.206	0.021	-0.039	4.35	0.223	0.029	-0.046	4.12	0.185	0.087	-0.050	4.12	0.182	0.085	-0.050	4.12	0.173	0.082	-0.047	4.26	0.193	0.202	-0.031	4.31	0.206	0.021	-0.039	
5.33	0.262	0.274	-0.040	5.41	0.269	0.021	-0.046	5.45	0.286	0.034	-0.050	5.16	0.239	0.104	-0.054	5.16	0.233	0.110	-0.053	5.15	0.215	0.093	-0.048	5.33	0.262	0.274	-0.040	5.41	0.269	0.021	-0.046	
6.43	0.292	0.368	-0.047	6.51	0.334	0.042	-0.061	6.56	0.367	0.046	-0.071	6.19	0.287	0.159	-0.076	6.18	0.280	0.161	-0.075	6.18	0.261	0.159	-0.069	6.43	0.292	0.368	-0.047	6.51	0.334	0.042	-0.061	
8.61	0.409	0.633	-0.063	8.72	0.487	0.076	-0.089	8.80	0.539	0.074	-0.126	8.26	0.392	0.233	-0.101	8.25	0.373	0.230	-0.099	8.24	0.343	0.208	-0.090	8.61	0.409	0.633	-0.063	8.72	0.487	0.076	-0.089	
10.77	0.516	0.956	-0.077	10.91	0.595	0.113	-0.106	11.02	0.682	0.118	-0.165	10.32	0.478	0.314	-0.125	10.32	0.459	0.317	-0.121	10.30	0.426	0.253	-0.110	10.77	0.516	0.956	-0.077	10.91	0.595	0.113	-0.106	
12.96	0.643	1.460	-0.094	13.11	0.706	0.166	-0.125	13.28	0.800	0.170	-0.202	12.38	0.570	0.397	-0.131	12.37	0.539	0.393	-0.124	12.37	0.508	0.371	-0.120	12.96	0.643	1.460	-0.094	13.11	0.706	0.166	-0.125	
15.14	0.764	2.023	-0.111	15.32	0.837	0.226	-0.149	15.46	0.940	0.231	-0.265	14.46	0.720	0.517	-0.157	14.46	0.680	0.513	-0.153	14.46	0.648	0.494	-0.147	15.14	0.764	2.023	-0.111	15.32	0.837	0.226	-0.149	
17.33	0.874	2.641	-0.123	17.46	0.905	0.293	-0.166									16.50	0.697	0.600	-0.159	16.48	0.648	0.494	-0.147	17.33	0.874	2.641	-0.123	17.46	0.905	0.293	-0.166	

$\alpha$	$C_L$	$C_D$	$C_M$	$\alpha$	$C_L$	$C_D$	$C_M$	$\alpha$	$C_L$	$C_D$	$C_M$	$\alpha$	$C_L$	$C_D$	$C_M$	$\alpha$	$C_L$	$C_D$	$C_M$	$\alpha$	$C_L$	$C_D$	$C_M$	$\alpha$	$C_L$	$C_D$	$C_M$	$\alpha$	$C_L$	$C_D$	$C_M$	
M=1.40 B=7.5x10°				M=1.53 B=7.5x10°				M=1.60 B=7.5x10°				M=1.70 B=7.5x10°				M=1.80 B=7.5x10°				M=1.90 B=7.5x10°				M=2.00 B=7.5x10°				M=2.10 B=7.5x10°				
-0.04	-0.002	0.0112	-0.001	-0.01	0.001	0.0107	-0.001	0	-0.002	0.0105	-0.001	0	-0.002	0.0104	-0.001	0	-0.002	0.0104	-0.001	0	-0.002	0.0104	-0.001	0	-0.002	0.0104	-0.001	0	-0.002	0.0104	-0.001	0
-6.53	-0.287	0.412	-0.074	-6.50	-0.287	0.391	-0.067	-6.48	-0.280	0.363	-0.066	-6.45	-0.276	0.336	-0.065	-6.45	-0.276	0.336	-0.065	-6.45	-0.276	0.336	-0.065	-6.53	-0.287	0.412	-0.074	-6.50	-0.287	0.391	-0.067	
-7.44	-0.236	0.316	-0.060	-7.41	-0.228	0.299	-0.077	-7.41	-0.219	0.282	-0.075	-7.38	-0.215	0.257	-0.074	-7.38	-0.215	0.257	-0.074	-7.38	-0.215	0.257	-0.074	-7.44	-0.236	0.316	-0.060	-7.41	-0.228	0.299	-0.077	
-8.35	-0.190	0.240	-0.046	-8.33	-0.180	0.230	-0.046	-8.32	-0.176	0.224	-0.044	-8.31	-0.172	0.209	-0.043	-8.31	-0.172	0.209	-0.043	-8.31	-0.172	0.209	-0.043	-8.35	-0.190	0.240	-0.046	-8.33	-0.180	0.230	-0.046	
-9.26	-0.144	0.185	-0.036	-9.25	-0.136	0.179	-0.034	-9.25	-0.134	0.173	-0.033	-9.23	-0.132	0.158	-0.032	-9.23	-0.132	0.158	-0.032	-9.23	-0.132	0.158	-0.032	-9.26	-0.144	0.185	-0.036	-9.25	-0.136	0.179	-0.034	
-10.18	-0.097	0.149	-0.025	-10.17	-0.092	0.144	-0.022	-10.16	-0.090	0.138	-0.021	-10.15	-0.088	0.132	-0.020	-10.15	-0.088	0.132	-0.020	-10.15	-0.088	0.132	-0.020	-10.18	-0.097	0.149	-0.025	-10.17	-0.092	0.144	-0.022	
-11.10	-0.050	0.126	-0.011	-11.10	-0.046	0.122	-0.011	-11.10	-0.044	0.118	-0.011	-11.10	-0.042	0.114	-0.011	-11.10	-0.042	0.114	-0.011	-11.10	-0.042	0.114	-0.011	-11.10	-0.050	0.126	-0.011	-11.10	-0.046	0.122	-0.011	
-12.02	-0.004	0.110	-0.001	-12.01	-0.003	0.109	0	-12.01	-0.004	0.107	0	-12.01	-0.004	0.105	0	-12.01	-0.004	0.105	0	-12.01	-0.004	0.105	0	-12.02	-0.004	0.110	-0.001	-12.01	-0.003	0.109	0	
1.06	0.070	0.024	-0.015	1.09	0.048	0.023	-0.014	1.08	0.046	0.018	-0.013	1.08	0.044	0.018	-0.013	1.08	0.044	0.018	-0.013	1.08	0.044	0.018	-0.013	1.06	0.070	0.024	-0.015	1.09	0.048	0.023	-0.014	
2.17	0.099	0.032	-0.027	2.17	0.094	0.018	-0.026	2.16	0.090	0.013	-0.024	2.16	0.086	0.013	-0.024	2.16	0.086	0.013	-0.024	2.16	0.086	0.013	-0.024	2.17	0.099	0.032	-0.027	2.17	0.094	0.018	-0.026	
3.26	0.146	0.090	-0.040	3.25	0.139	0.016	-0.037	3.24	0.134	0.019	-0.036	3.24	0.130	0.019	-0.036	3.24	0.130	0.019	-0.036	3.24	0.130	0.019	-0.036	3.26	0.146	0.090	-0.040	3.25	0.139	0.016	-0.037	
4.34	0.193	0.247	-0.054	4.33	0.183	0.023	-0.049	4.32	0.177	0.021	-0.048	4.32	0.173	0.021	-0.048	4.32	0.173	0.021	-0.048	4.32	0.173	0.021	-0.048	4.34	0.193	0.247	-0.054	4.33	0.183	0.023	-0.049	
5.43	0.241	0.392	-0.061	5.41	0.227	0.030	-0.060	5.40	0.219	0.033	-0.059	5.40	0.215	0.033	-0.059	5.40	0.215	0.033	-0.059	5.40	0.215	0.033	-0.059	5.43	0.241	0.392	-0.061	5.41	0.227	0.030	-0.060	
6.52	0.289	0.411	-0.076	6.50	0.270	0.035	-0.070	6.48	0.262	0.033	-0.068	6.48	0.258	0.033	-0.068	6.48	0.258	0.033	-0.068	6.48	0.258	0.033	-0.068	6.52	0.289	0.411	-0.076	6.50	0.270	0.035	-0.070	

NACA



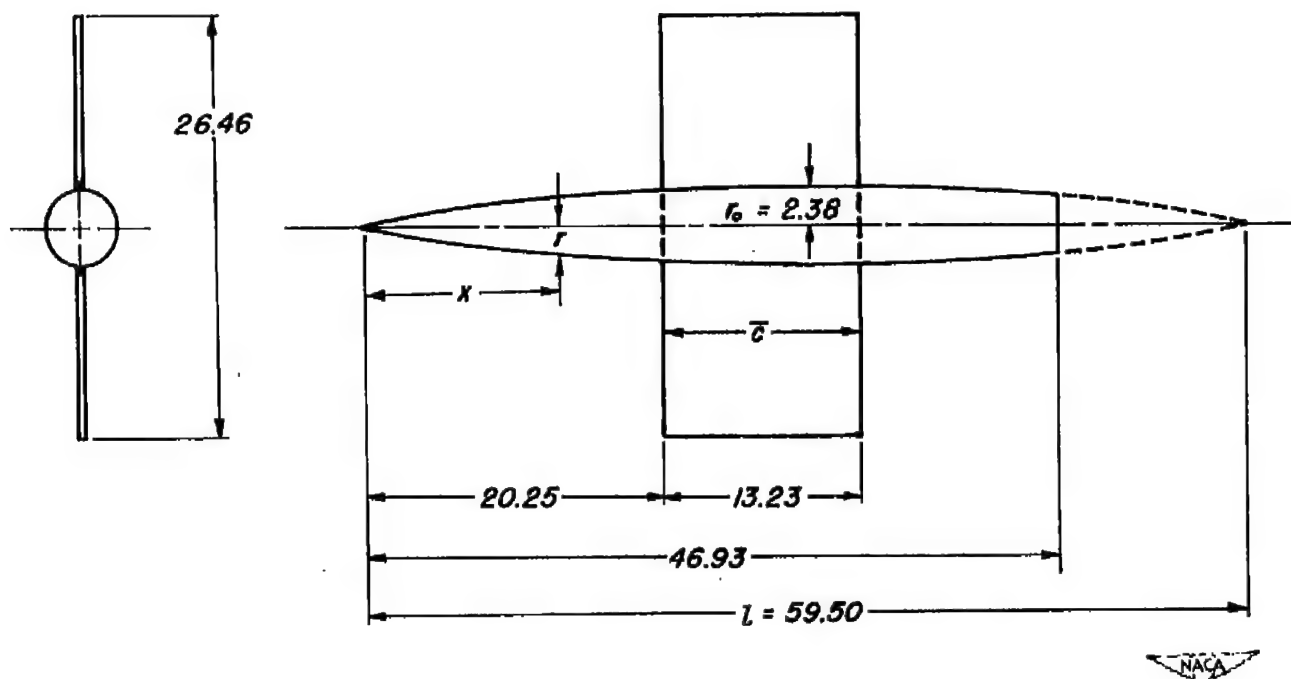
NACA RM A52LO2



Equation of fuselage radii:

All dimensions shown in inches.

$$\frac{r}{r_0} = \left[ 1 - \left( 1 - \frac{2x}{l} \right)^2 \right]^{\frac{3}{4}}$$



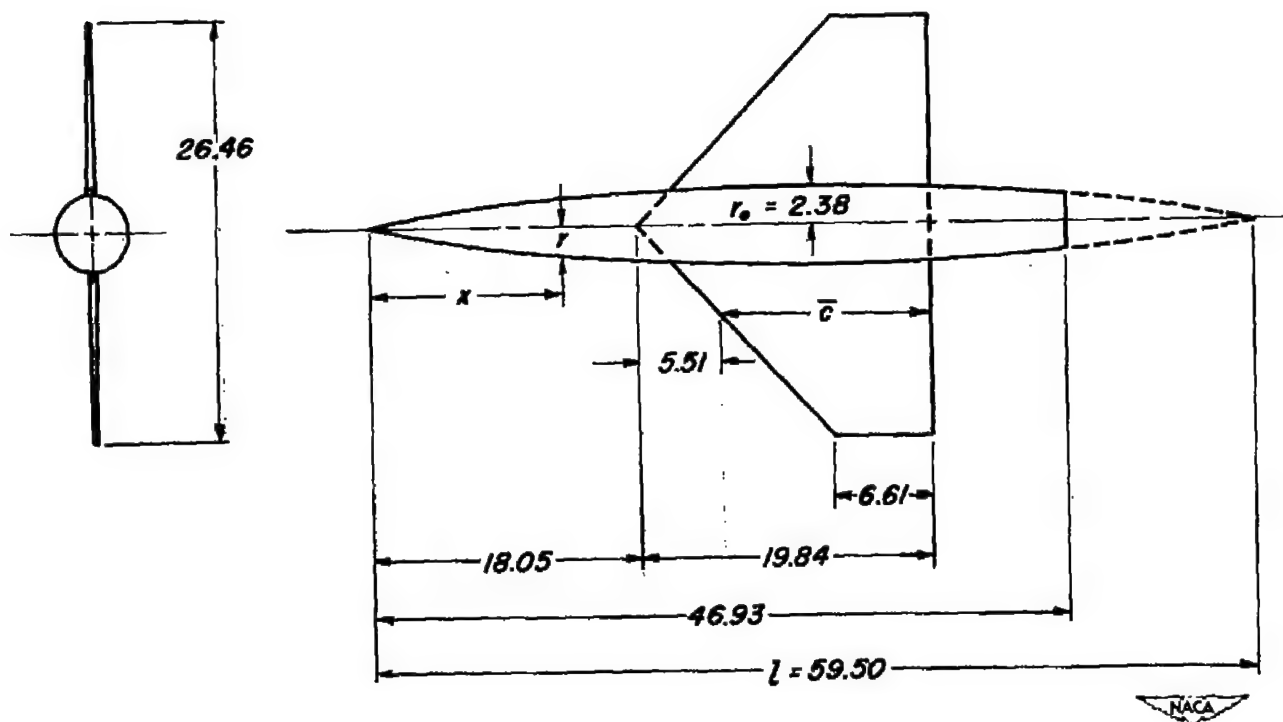
(a) Rectangular wing model.

Figure 1.-Plan and front views of the rectangular, swept-back, and triangular wing models.

Equation of fuselage radii:

$$\frac{r}{r_0} = \left[ 1 - \left( 1 - \frac{2x}{l} \right)^2 \right]^{\frac{3}{4}}$$

All dimensions shown in inches.



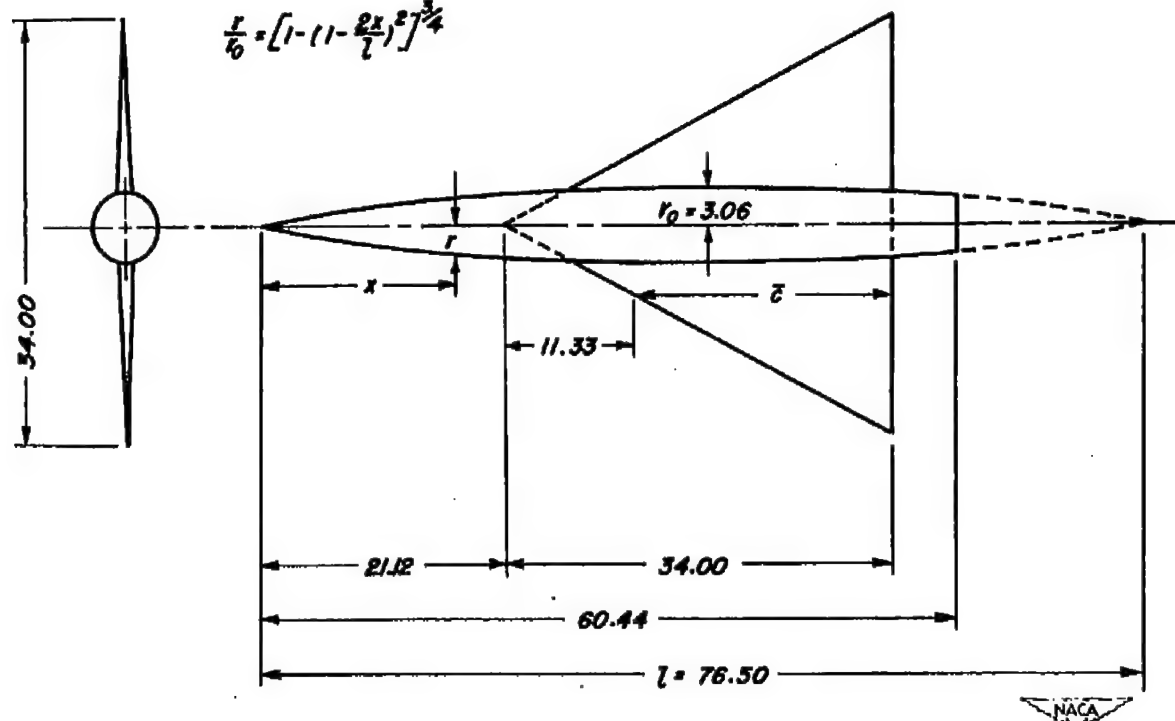
(b) Swept-back wing model.

Figure 1.- Continued.

Equation of fuselage radii:

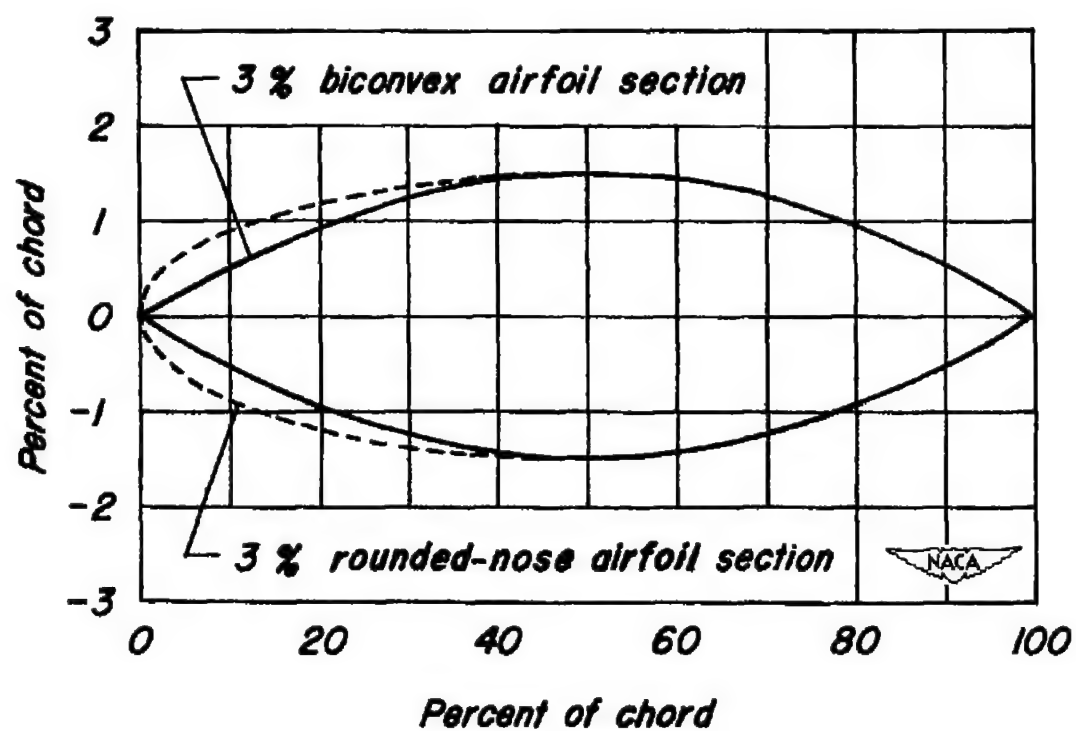
All dimensions shown in inches.

$$\frac{r}{r_0} = \left[ 1 - \left( 1 - \frac{2x}{l} \right)^2 \right]^{\frac{3}{4}}$$

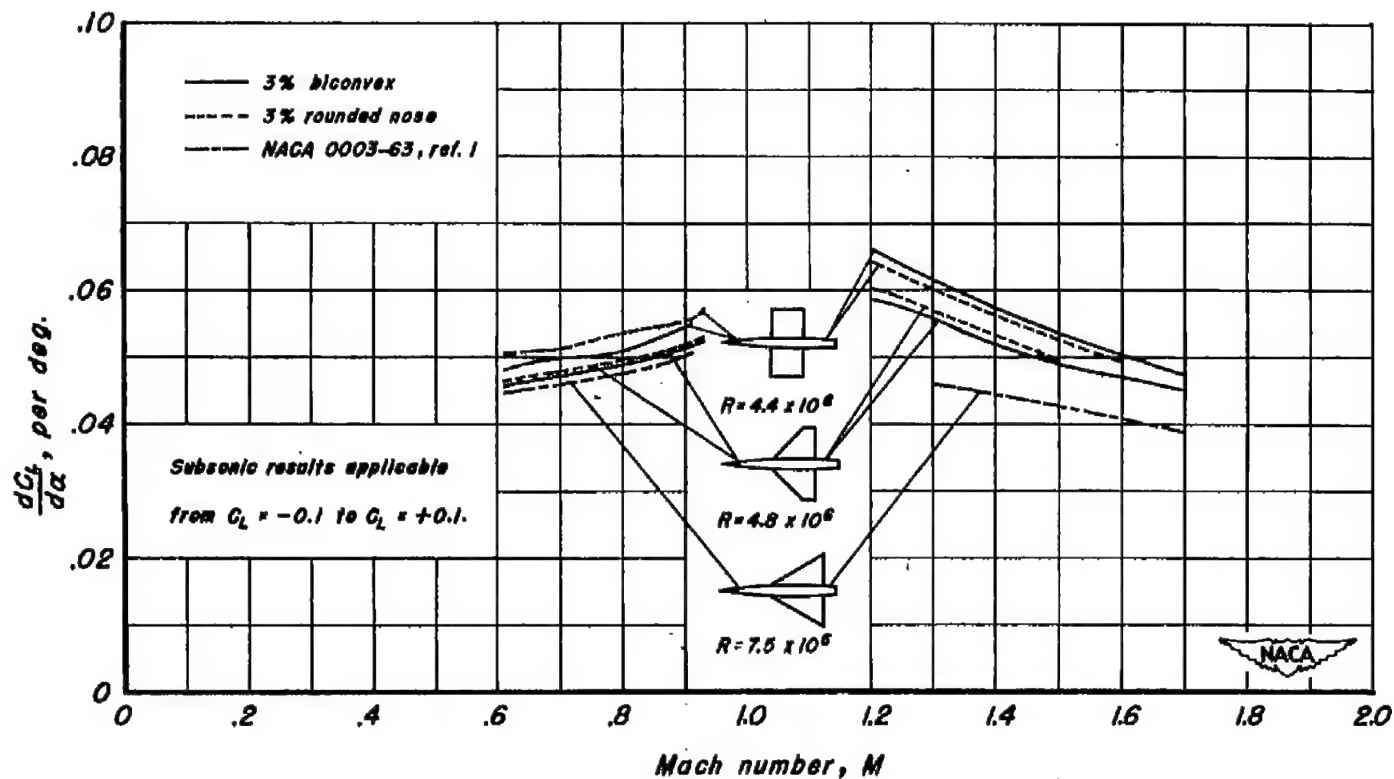


(c) Triangular-wing model of reference 1.

Figure 1.- Concluded.

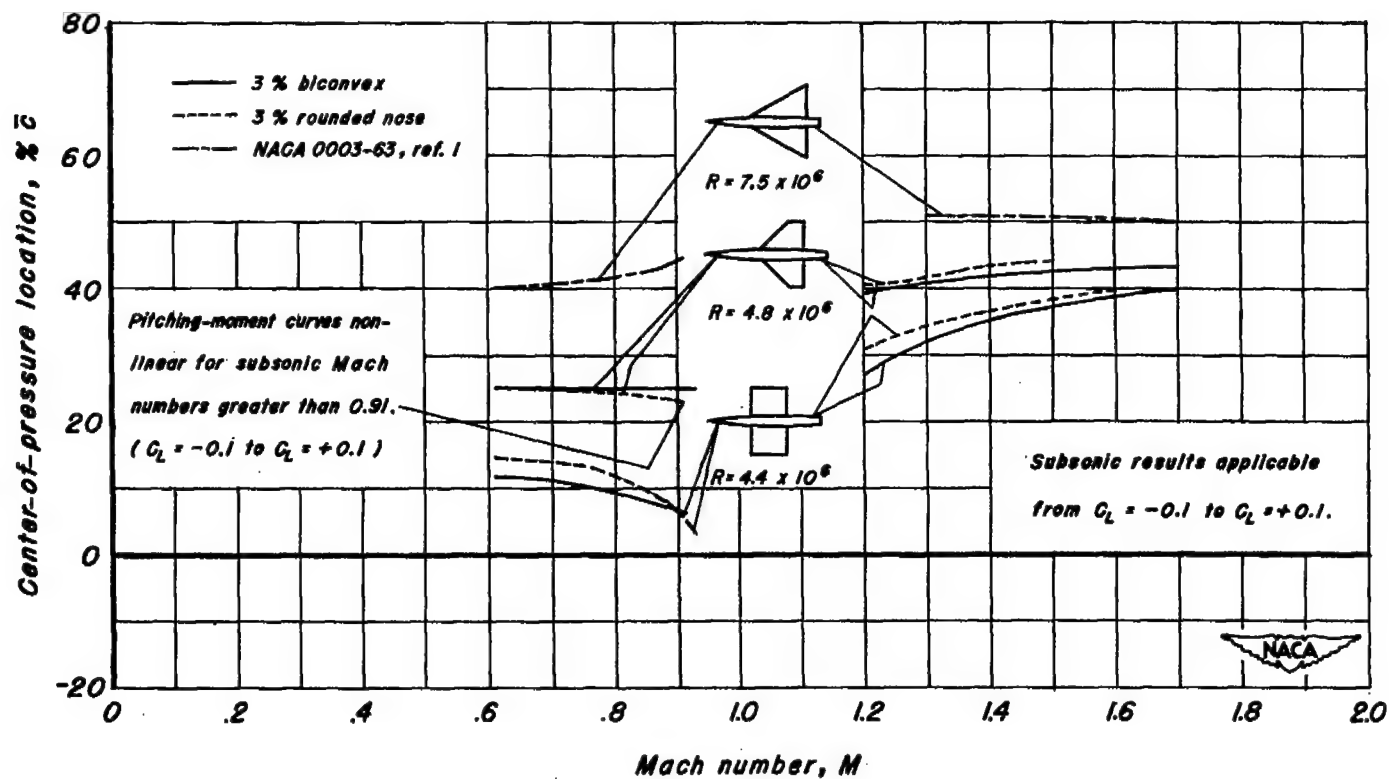


*Figure 2.- Comparison of the biconvex airfoil section with the rounded-nose airfoil section.*



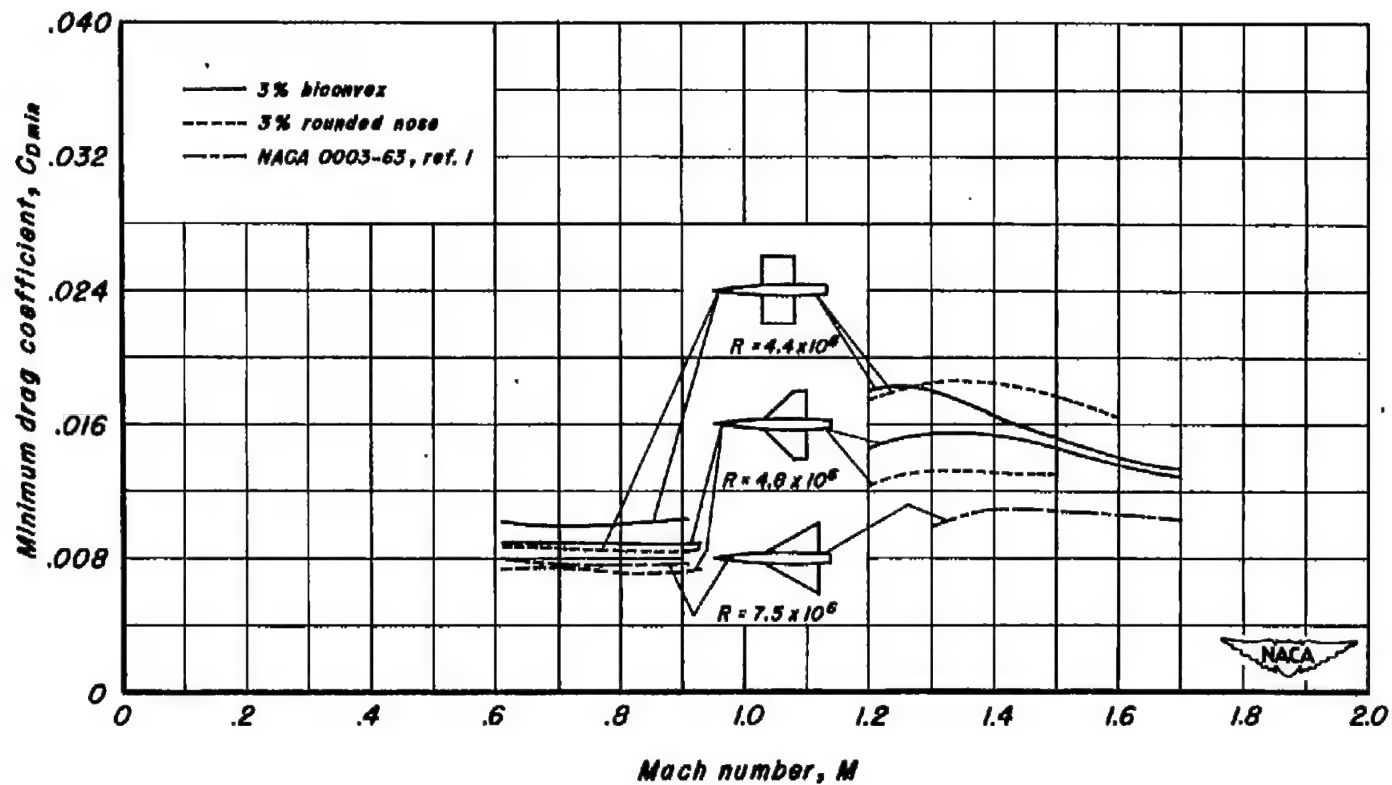
(a) Lift-curve slope.

Figure 3.— Effects of plan form and airfoil thickness distribution on various aerodynamic parameters.



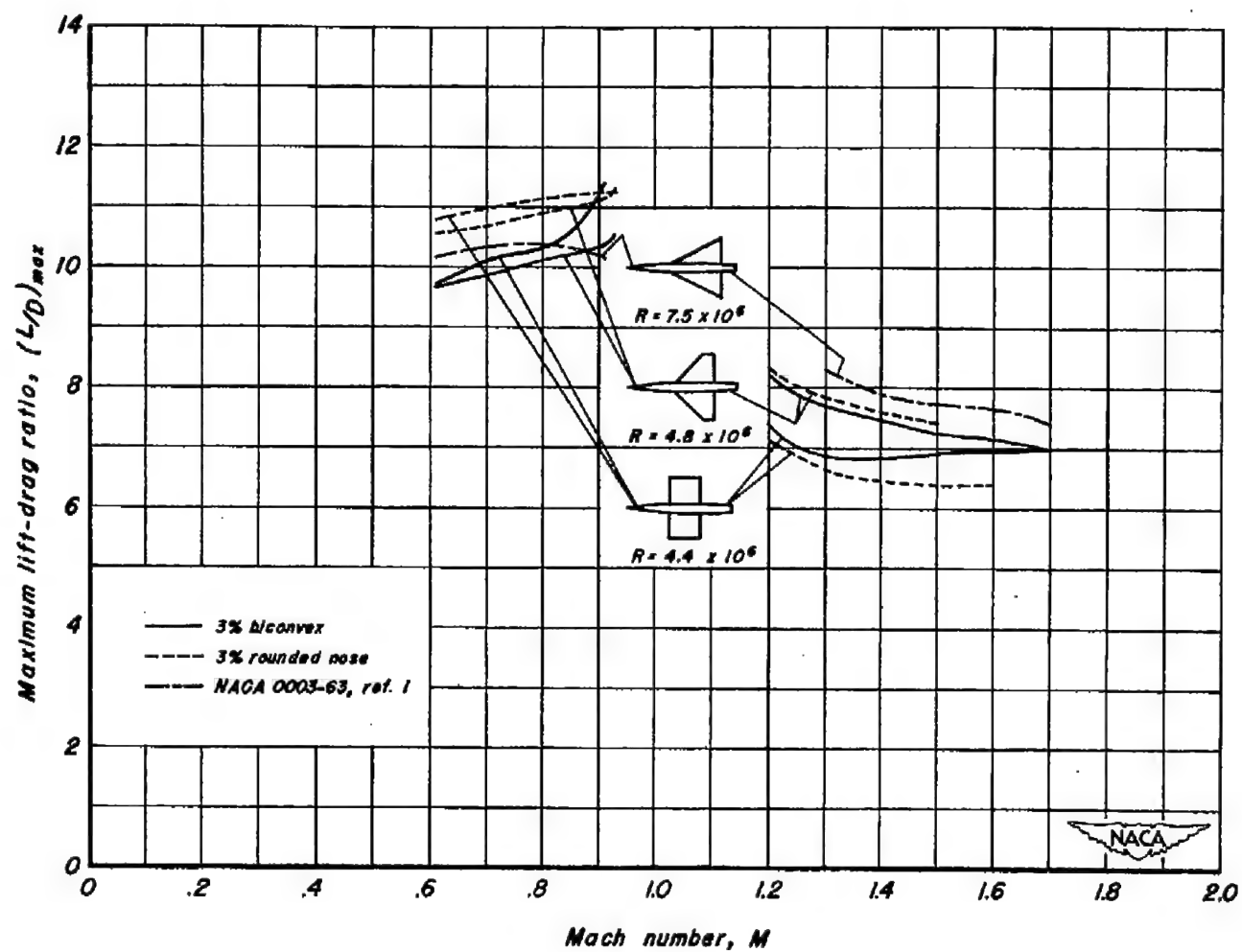
(b) Center-of-pressure location.

Figure 3.- Continued.



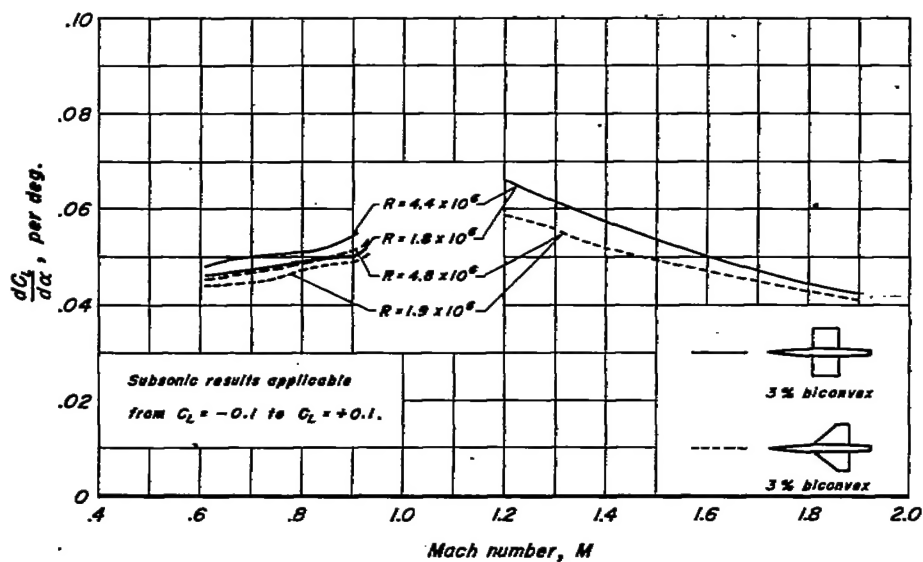
(c) Minimum drag coefficient.

Figure 3.- Continued.

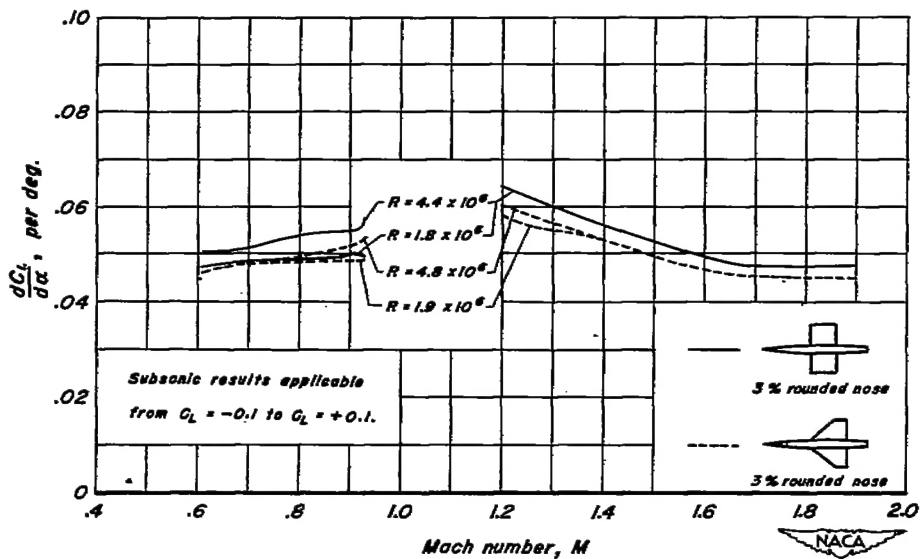


(d) Maximum lift-drag ratio.

Figure 3.- Concluded.

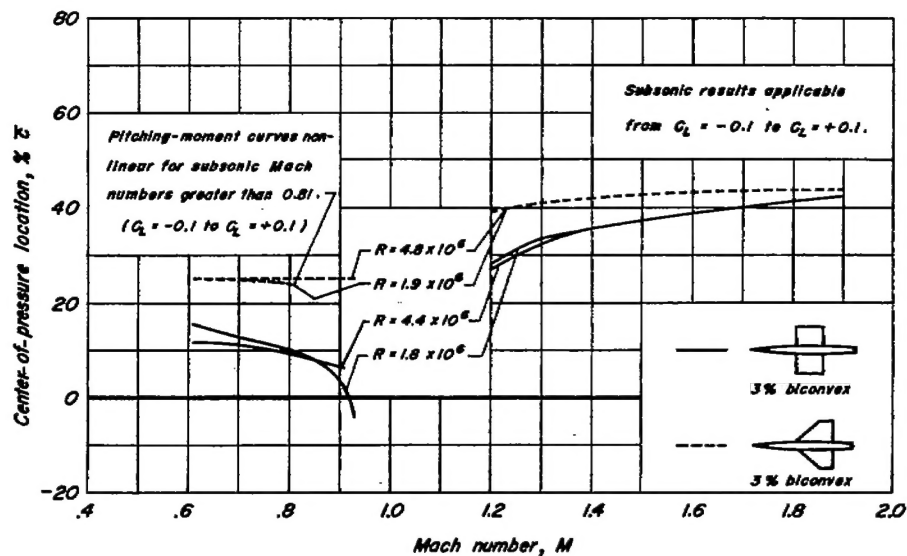


(a) Sharp leading edges.

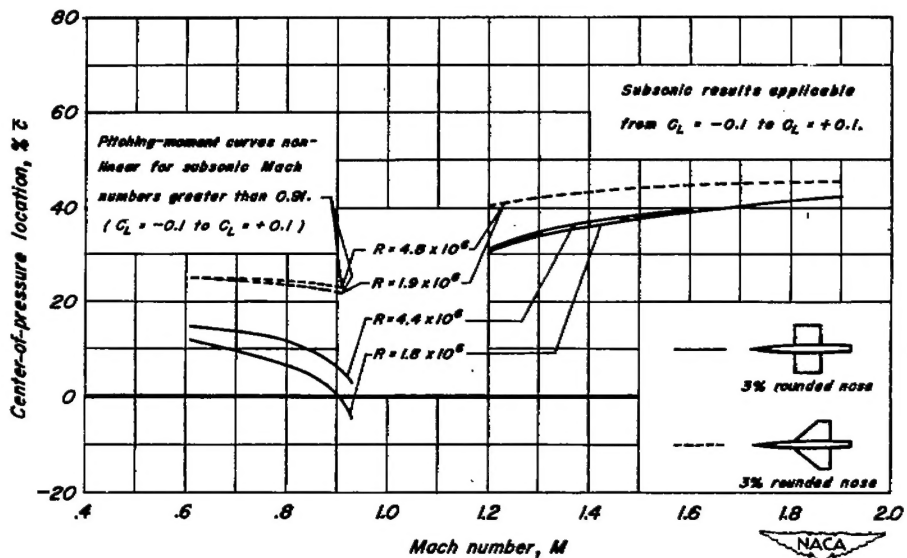


(b) Rounded leading edges.

Figure 4.—Effects of Reynolds number on the lift-curve slopes of wings with sharp and rounded leading edges.

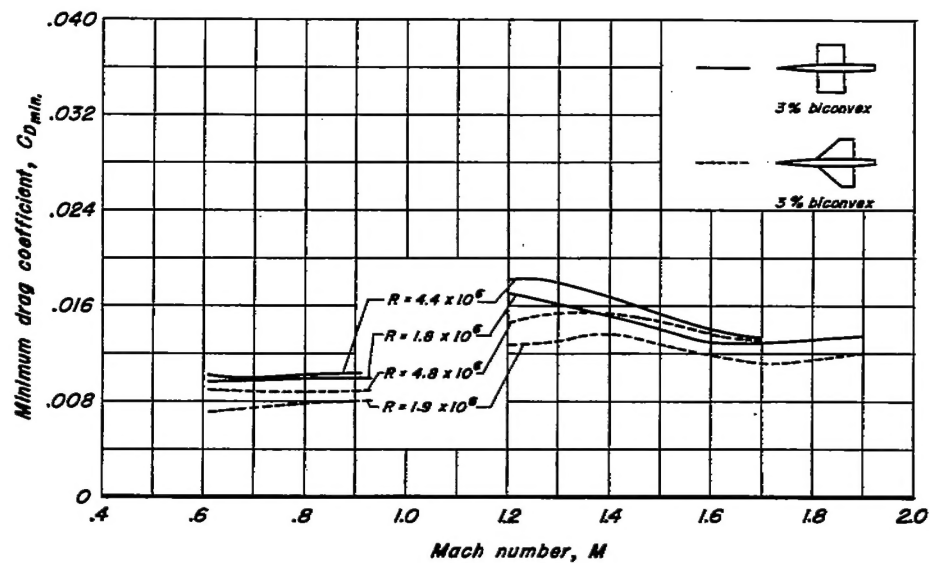


(a) Sharp leading edges.

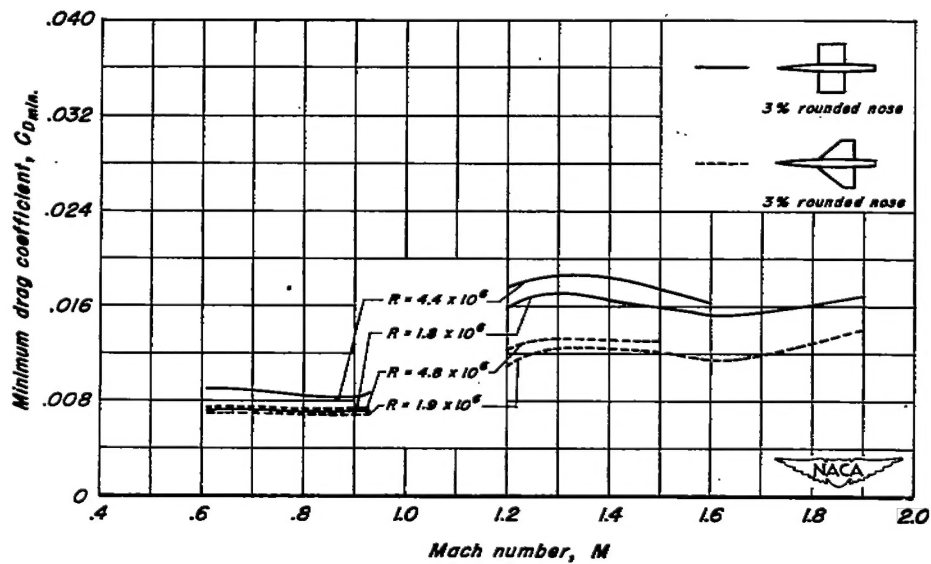


(b) Rounded leading edges.

Figure 5.—Effects of Reynolds number on the center-of-pressure locations of wings with sharp and rounded leading edges.

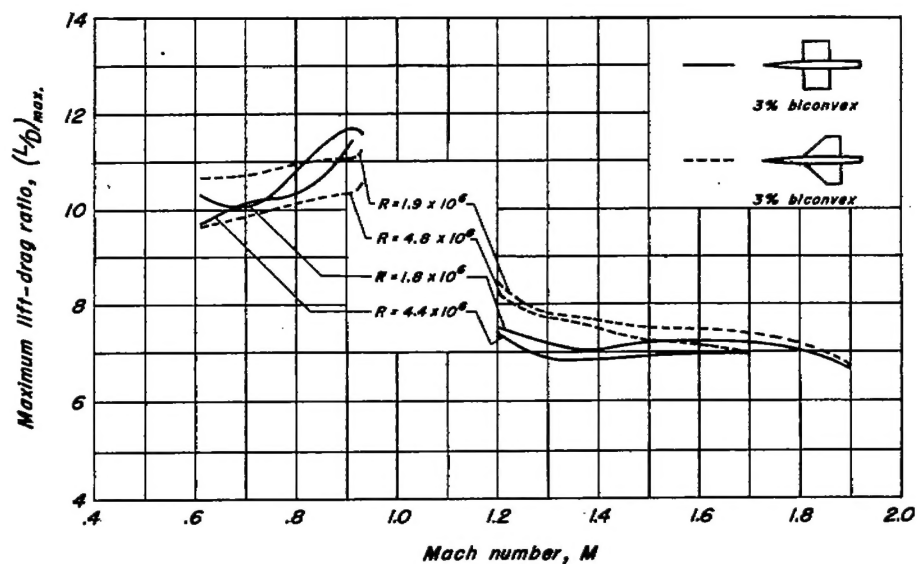


(a) Sharp leading edges.

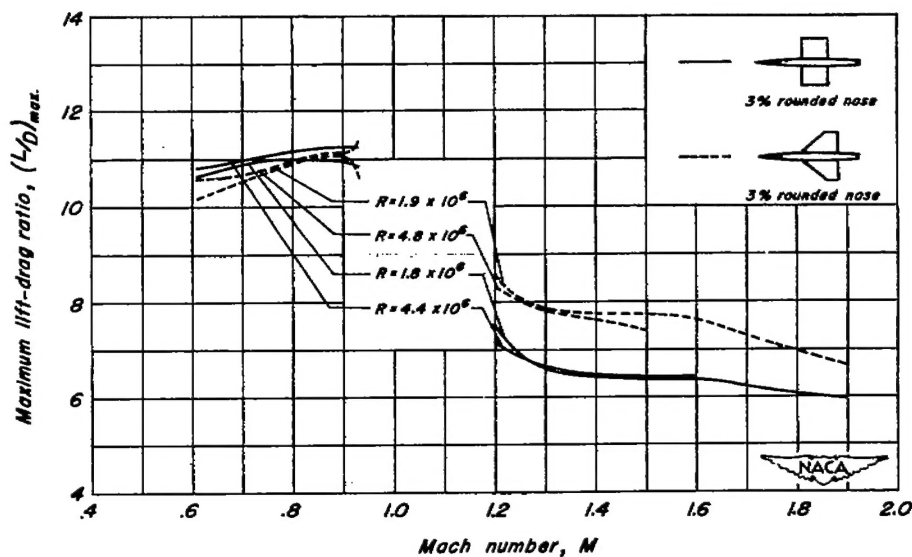


(b) Rounded leading edges.

Figure 6.- Effects of Reynolds number on the minimum drag coefficients of wings with sharp and rounded leading edges.



(a) Sharp leading edges.



(b) Rounded leading edges.

Figure 7.-Effects of Reynolds number on the maximum lift-drag ratios of wings with sharp and rounded leading edges.